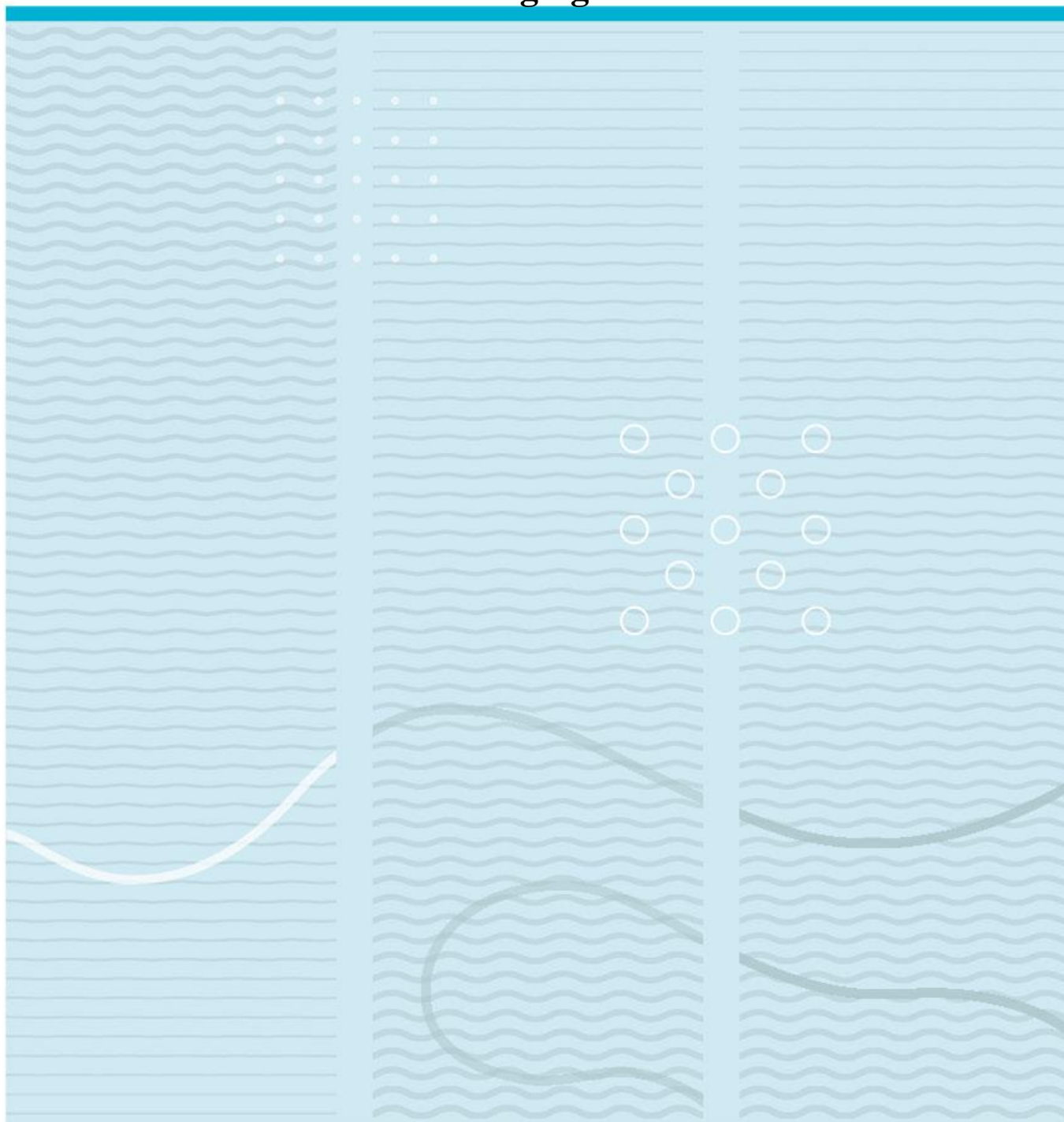Marte Roti

Prevalence of optic disc drusen in a Norwegian population measured with multimodal imaging

University of South-Eastern Norway

Faculty of Health and Social sciences

Department of optometry, radiography, and lighting design

PO Box 235

NO-3603 Kongsberg, Norway

http://www.usn.no

This thesis is worth 30 study points

Summary

Purpose

This study investigates the prevalence of optic nerve head drusen (ONHD) in a Norwegian population using different imaging methods; optical coherence tomography (OCT), autofluorescence (AF)-imaging and fundus photography – and further looks at some of the characteristics of the ONHD and its effect on the retinal nerve fiber layer (RNFL).

Methods

This is a cross sectional study where subjects above 18 visiting an optometric practice were recruited consecutively. The subjects who participated underwent an optometric examination that included SD-OCT, fundus photography and AF-images (Optomap). The images from both eyes were analysed and the presence, location and size of ONHD were registered. The size of ONHD was measured only in the OCT-images. Cohen's kappa was used to analyse the interrater reliability between the imaging methods, and differences between groups were analysed with Welch's ANOVA and independent T-test, and a p-value <0.05 was considered significant.

Results

305 subjects were included with a mean age of 45.41 ($\pm$ SD 14.73) where 61.3% were women. ONHD was prevalent in 23 (7.5% [CI 4.8-11%]) of subjects identified with SD-OCT; 10 (3.3% [CI 1.6-5.9%]) of subjects identified with fundus photography; 22 (7.2% [CI 4.6-10.7%]) of subjects identified with AF-imaging. The mean age of subjects identified with ONHD measured with OCT was 41.8 years (SD $\pm$12.87) where 69.9% were female. ONHD were bilateral in 60.9% of these cases.

AF-imaging compared to OCT had a sensitivity of 89.5% (Kappa=0.94) and 77.8% (Kappa=0.87) of right (RE) and left (LE) eyes respectively. Fundus photography compared to OCT had a sensitivity of 31.6% (Kappa=0.46) and 44.4% (Kappa=0.601) of RE and LE respectively.

When measuring the ONHD diameter with OCT, those who were not visible on AF-images (non-hyperautofluorescent) had a significantly smaller diameter compared to the diameter of the hyperautofluorescent ONHD (p<0.023 RE and p<0.001 LE). The clinically visible ONHD had a larger diameter than the buried ONHD (p<0.05 for both eyes).

ONHD were least present in the temporal quadrant of the ONH for all imaging methods.

The global RNFL thickness were thinner in eyes with ONHD compared to the normal group (p<0.051 RE and p<0.075LE). Eyes with visible ONHD had thinner RNFL than eyes with buried ONHD (p<0.013 and p<0.056 for RE and LE respectively). The RNFL was thicker in left eyes with non-hyperautofluorescent ONHD than eyes with hyperfluorescent ONHD, for right eyes there was no correlation (p<0.26) but there was only one eye with non-hyperfluorescent ONHD for right eyes.

The different ONHD diameter did not have a significant effect on RNFL (p=0.180 RE and p=0.119 LE). Increase in ONHD quantity did decrease the RNFL in right eyes (p<0.005), but for left eyes there was no significant decrease (p=0.151). There was no correlation between disc diameter between groups with or without ONHD (p=0.272 for right eyes and p=0.812 for left eyes).

Conclusion

The prevalence of ONHD found in this study is higher than previously reported in the literature, although a larger sample size is warranted to transfer these numbers to the whole Norwegian population. The disc diameter did not show any correlation with the prevalence. Increased quantity of ONHD had larger effect on the RNFL than increased ONHD diameter.

Autofluorescent imaging (AF) and SD-OCT have a high correlation where AF-imaging detects all the visible ONHD and the majority of the buried ONHD. Still, there may be some buried ONHD that are only detected with OCT, but these are expected to be of less clinical importance since they are both smaller and have less impact on the RNFL. Thus, AF and SD-OCT are imaging techniques that both have a high clinical value when diagnosing optic nerve head drusen.

Key words: Optic nerve head drusen, optic disc drusen, SD-OCT, AF-imaging, fundus photography

Contents

Foreword

The process of writing this thesis has of course been challenging at times, but mainly fun. The fun part would not have been possible without the support from people around me.

I would like to thank

- Supervisor Tove Lise Morisbakk, for all advice, assistance and encouragement.
- Co-supervisor Per Olof Lundmark for help with statistical issues.
- Colleagues Kristine Høydal and Trude Nygard Johansen, for help with data collection.
- Employer Krogh Optikk, for their flexibility and support.
- Fellow peers, for making the master's degree enjoyable!
- Family, friends and my boyfriend Robert Kresz, for all the love and support.

Oslo, 12th of May 2020

Marte Roti

1 Introduction

The use of optical coherence tomography (OCT) among Norwegian optometrists is expanding, which in turn leads to better possibilities to make more accurate diagnoses in cases of atypical nerve heads, like optic nerve head drusen (ONHD).

Not all ONHD are visible with ophthalmoscopy or fundus photography, and the ONHD that are located deeper in the optic disc may therefore be more difficult to detect. The buried ONHD may also give the optic disc a swollen appearance, which makes it challenging to differentiate from the potentially harmful optic disc edema (ODE). The ONHD may lead to reduced visual function due to the compressive effect on the retinal nerve fibre layer (RNFL). This study will investigate different imaging modules in detection of ONHD in a Norwegian population.

1.1 Optic nerve head drusen

Optic nerve head drusen (ONHD) are acellular deposits with calcified borders that forms within the optic nerve head (Hamann, Malmqvist, & Costello, 2018; A. G. Lee & Zimmerman, 2005). The prevalence of ONHD varies from 0.2% to 0.3% in clinical studies (Lorentzen, 1966; You, Xu, Wang, & Jonas, 2009) to 1.8% to 2.04% in histological studies (Friedman, Gartner, & Modi, 1975; Skougaard, Heegaard, Malmqvist, & Hamann, 2019) and 1% to 14.6% in studies using OCT (Ghassibi et al., 2017; Malmqvist et al., 2017c). In the clinical studies the ONH was only visually examined either by ophthalmoscopy or photography (Lorentzen, 1966; You et al., 2009). The different prevalence between clinical- and histopathological studies suggests that only around 15% of the drusen are clinically visible and the rest is buried deeper within the optic nerve head. ONHD occur more often in female patients than male patients, 60% and 40% respectively, and bilateral in 61-95% of cases (Gili, Flores-rodríguez, Martin-ríos, & Carrasco Font, 2013; Malmqvist et al., 2017c; Malmqvist, Lindberg, Dahl, Jørgensen, & Hamann, 2017).

The ONHD are always located anterior to the lamina cribrosa (Auw-Haedrich, Staubach, & Witschel, 2002; Hamann et al., 2018), the size varies between 5 to 1000 μm (Tso, 1981), and the mean greatest diameter is around 686.8 μm (Sato, Mrejen, & Spaide, 2013). The pathophysiology is not clear, but several mechanisms are proposed; impaired axonal transport, axonal disruption, extrusion of mitochondria into the extracellular space and continuous

calcium deposition (Hamann et al., 2018; Lorentzen, 1966; Tso, 1981). The ONHD is likely to cause mechanical stress on prelaminar structures in the scleral canal leading to axonal degradation and ganglion cell death, which further results in reduced retinal sensitivity and visual field defects (Hamann et al., 2018).

Due to the pathophysiological theories, it is suggested that the ONHD is a result of a small scleral canal size, but the results are conflicting. Floyd, Katz, and Digre (2005) concluded that scleral canal size probably is not an etiologic factor in the development of ONHD. Another study found larger scleral canal size in ONHD subjects measured with OCT, but in the same study they found a smaller scleral canal size in ONHD subjects measured with fundus (Flores-Rodríguez, Gili, Martín-Ríos, & Grifol-Clar, 2013). This suggests a low degree of correlation between the two methods as stated by (Hamann et al., 2018). A more recent study on ONH in children (mean age: 11.4 years) found significantly smaller scleral canal size in eyes with ONHD (Malmqvist et al., 2017c).

The ONHD are situated in the prelaminar region in the scleral canal and are either located deep or more superficial (Malmqvist, Bursztyn, et al., 2017). The superficial ONHD are visible with ophthalmoscopy or by photography, and the buried are only detected with OCT or B-scan ultrasound if the ONHD margin is calcified (Malmqvist, Lindberg, et al., 2017). It has been found that the visible ONHD have a larger volume than the buried ONHD (Malmqvist, Lindberg, et al., 2017). If visible, they appear as globular bodies that protrude from the Optic Nerve Head (ONH) and may give the ONH an irregular and uneven appearance (Roh et al., 1998). A histological study with a large study sample of 1713 eyes, found that 23% of cases has superficial ONHD, which was defined as anterior to Bruch's membrane (Skougaard et al., 2019). Another study, conducted on subjects <18 years, found visible ONHD in 21% of the study sample (Teixeira, Marques, Mano, Couceiro, & Pinto, 2019).

The appearance of a disc with buried ONHD could be variable and range from near normal to optic disc edema, with hazy disc margins and anomalous blood-vessel branching over the disc (Katz & Pomeranz, 2006; Lam, Morais, & Pasol, 2008). Diagnosing correctly is important to avoid unnecessary work-up and to avoid missing potentially serious conditions such as papilledema, which could be a manifestation of raised intracranial pressure (Lam et al., 2008). Because of the anomalous appearance in buried ONHD it is often mistaken to be papilledema, and in a study concerning suspected papilledema in children, 52% were misdiagnosed with papilledema and 34.6% of these had ONHD as the last diagnose (Liu, Murphy, Mercer, Tychsen, & Smyth, 2014). Buried drusen are more prevalent in children and it is thought that

ONHD gets more visible with age either from drusen growth, increase in drusen number, drusen migration or age-related thinning of the overlying retinal nerve fibre layer (RNFL) so the visibility increases and typically develops from buried to superficial ONHD at 12 years of age (Hoover, Robb, & Petersen, 1988). It is also proposed that the number and size of ONHD progress most rapidly during the teenage years (Frisén, 2008; Malmqvist, Lund-Andersen, & Hamann, 2017). A long-term study over 56 years, found minimal progression in size and number of the clinically visible ONHD, and minimal progression in visual field defects, supporting the theory about rapid progression in the teenage years (Malmqvist, Lund-Andersen, et al., 2017). The age range of the subjects when the first study was conducted was 13 to 22 years and a mean of 16 years (Lorentzen, 1966; Malmqvist, Lund-Andersen, et al., 2017).

There are several ocular and systemic diseases that have been found in association with ONHD, but the only anomalies that truly is associated with ONHD are retinitis pigmentosa, angioid streaks with or without pseudoxanthoma elasticum and Alagille Syndrome (Auw-Haedrich et al., 2002; El-Koofy et al., 2011).
These co-conditions will not be addressed further in this study.

1.2 Imaging techniques

1.2.1 OCT Technology

Optical Coherence Tomography (OCT) is a non-invasive imaging technique that obtains cross-sectional information from the structures in the eye/retina. OCT is increasingly used in optometric practice, where the OCT with spectral domain (SD) technology is mostly distributed among optometrists. Mainly ophthalmologists, in addition to some optometrists, use the newer Swept Source-OCT (SS-OCT) technology. Enhanced Depth Imaging (EDI)-OCT or Swept Source OCT is now the preferred technique for detecting ONHD as it has proven to be more reliable because of improved visualization and higher resolution of the deeper layers of the optic nerve head (Merchant et al., 2013), and recent studies use OCT to confirm ONHD diagnosis (Malmqvist, Lund-Andersen, et al., 2017).
The clinical model Maestro OCT-1 from Topcon (Japan) that is used in the present study, is a SD-OCT with integrated fundus camera (Chaglasian et al., 2018). This model is highly distributed among Norwegian Optometrists. It is a non-contact OCT introduced in 2013 with a

high degree of automatic alignment, focus and capture, and provides an in-depth resolution is 6 μm (Chaglasian et al., 2018).

One disadvantage with the Maestro OCT-1 is that it is not possible to move the focal point deeper down to the choroidal level (which would have made it an EDI-OCT). This reduces the penetration to the deeper structures resulting in lack of information. An experimental way to get a sharper focus on the targeted area could be to turn the picture inverted/upside down, this is not performed in this study due to the inconvenience.

1.2.2 ONHD measured with OCT

With OCT, the ONHD are visualized as a mass with a signal-poor (hyporeflective) core surrounded by a hyperreflective margin, often containing hyperreflective foci (Hamann et al., 2018; Sato et al., 2013; Wang, Leong, Gale, & Wells, 2018). Examples of ONHD are illustrated in figure 1. Several small ONHD may also coalesce into larger conglomerates of ONHD and are either seen as the hyperreflective foci within the hyporeflective mass or as clustered hyperreflective spots in the ONH (Figure 1) (Malmqvist, Bursztyn, et al., 2017). The internal reflectivity of these spots is assumed to be fragments of calcified ONHD margins (Malmqvist, Bursztyn, et al., 2017). In studies using time domain-OCT (older OCT-technology) and SD-OCT, the integrity of the hyperreflective margin, mainly posterior, is often incomplete (Yi et al., 2009). This is due to the reduced penetration in the tissue compared to what is possible to achieve with EDI-OCT and SS-OCT described in the previous chapter. For SD-OCT, which is used in this study, the quality of the OCT-scan is found to be significantly improved when averaging 4 or more frames compared to only one frame used in a standard volume scan (Sakamoto, Hangai, & Yoshimura, 2008).
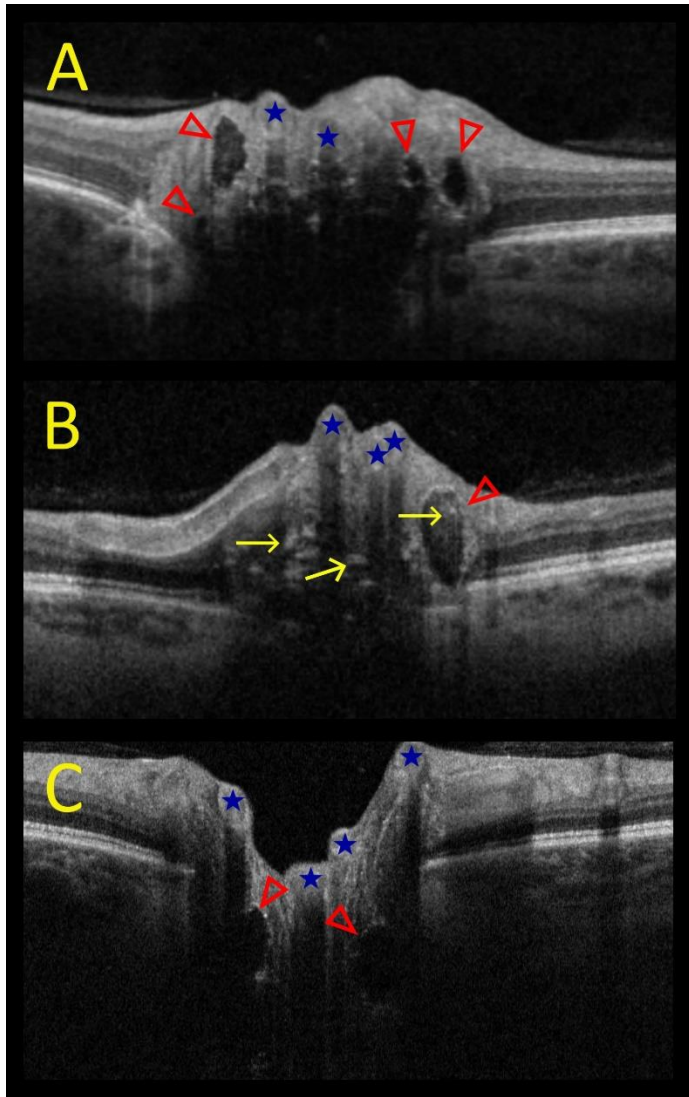
Figure 1: ONHD with OCT

OCT-scans of ONH from participants in the present study. ONHD show as hyporeflective mass with hyperreflective margin (red arrowheads). In some cases, there are hyperreflective foci (yellow arrows) within the hyporeflective mass or as conglomerates with no visible surrounding hyporeflectivity. Blood vessels causing posterior shadowing are marked with blue stars. (A=right eye, id.nr.105, B=right eye, id.nr.35, C=right eye, id.nr.46.)

In studies using EDI-OCT there have been reported findings of horizontal hyperreflective bands in relation to ONHD, and suggested as an indicator of drusen in evolution giving a higher prevalence (14.6%) (Ghassibi et al., 2017; Merchant et al., 2013). There is uncertainty if these hyperreflective bands are evolved to ONHD or are early signs of ONHD, as they may be

conglomerates of small ONHD (Ghassibi et al., 2017). In the absence of verification from follow-up studies, these lines are recommended not to classify as ONHD (Hamann et al., 2018).

There is an ongoing debate about the morphology of buried ONHD; whether the hyperreflective mass (Fig.4) described by (Chang & Pineles, 2016; Gospe, Bhatti, & El-Dairi, 2016; K. M. Lee, Woo, & Hwang, 2011; Rebolleda et al., 2015) as buried ONHD, located posterior to the outer plexiform and the outer nuclear layer, is ONHD or not. This mass is by several researchers described as peripapillary hyperreflective ovoid mass-like structures (PHOMS) (Hamann et al., 2018; Malmqvist, Sibony, et al., 2018; Wang et al., 2018), and similar findings are reported by histological studies where the masses are described as 'localized peripapillary axonal distension' (LPAD), which are considered the equivalent to PHOMS due to the identical morphology and localization (Skougaard et al., 2019).

It is suggested that PHOMS is displaced nerve fibres due to congestion in the prelaminar nerve head, either from large ONHD or a manifestation of an earlier edema - which makes it a marker of axoplasmic stasis (Malmqvist, Bursztyn, et al., 2018; Skougaard et al., 2019). PHOMS is found in 48% of eyes with resolved papilledema, but also found in healthy eyes (Gospe et al., 2016; Malmqvist, Sibony, et al., 2018). In relation to ONHD, it may coexist (id 27), but there is no evidence this is ONHD or will evolve to ONHD and therefore should not be diagnosed as ONHD (Malmqvist, Sibony, et al., 2018; Wang et al., 2018).
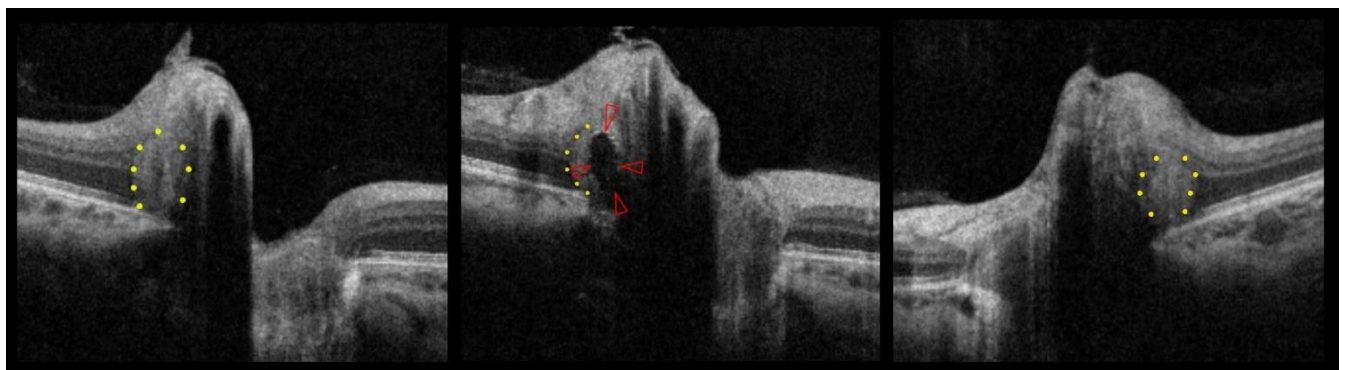

Figure 2: PHOMS vs ONHD

All images show OCT-scan of ONH assessed in this study. Left and middle (left eye, id nr.27) and right (right eye, id nr. 251). The peripapillary hyperreflective ovoid mass-like structures

(PHOMS) is outlined with yellow dots on all OCT-scans. Coexisting ONHD marked with red arrowheads (middle). There is no evidence these masses are ONHD.

OCT is a well-established tool for measuring the retinal nerve fiber layer (RNFL) and for documenting changes in the RNFL thickness. The RNFL defects are often indicated by the colours yellow and red to illustrate if they are outside the 95% and 99% normal limit of the normative database (Kim, Ahn, & Kim, 2013). Several studies reports thinner RNFL thickness in eyes with visible ONHD compared to eyes with buried ONHD (Gili, Flores-rodríguez, Martin-ríos, et al., 2013; Roh et al., 1998). There is also found significant thinning of the RNFL thickness both with increasing diameter of ONHD (Sato et al., 2013), and increasing quantity of ONHD (Roh et al., 1998). More recent studies, where actual ONHD volume was calculated, found significant thinning of the RNFL thickness and increase in visual field defects as the ONHD volume increased, independent of the vertical location (Malmqvist, Lindberg, et al., 2017; Skaat et al., 2017). It is suggested by Casado et al. (2014) and Malmqvist, Lindberg, et al. (2017) that measurement of ganglion cell-inner-plexiform layer (GCIPL) is more useful for detecting early damages in eyes with ONHD than the RNFL exam.

1.2.3 Fundus photography

The ONH of an eye with visible ONHD will, with fundus photography or ophthalmoscopy, have bright, irregular deposits and in many cases have an uneven disc margin (Lorentzen, 1966) as shown in *Figure 3*. The buried ONHD will not be visible but might make the ONH seem elevated and its margins obscured, which further could make it difficult to differentiate from papilledema. A previous study comparing imaging methods, found that 30.8% of eyes with ONHD had visible ONHD (Sato et al., 2013). The fundus colour photo is the most common, but monochromatic photography (red- or green free filter) has shown increased sensitivity in diagnosing ONHD compared to colour photography, where the ONHD will appear as rounded-looking bubbles on the monochromatic photo (Gili, Flores-Rodríguez, Yangüela, Orduña-Azcona, & Martín-Ríos, 2012). In the present study there is only used regular photography as shown on Figure 3.
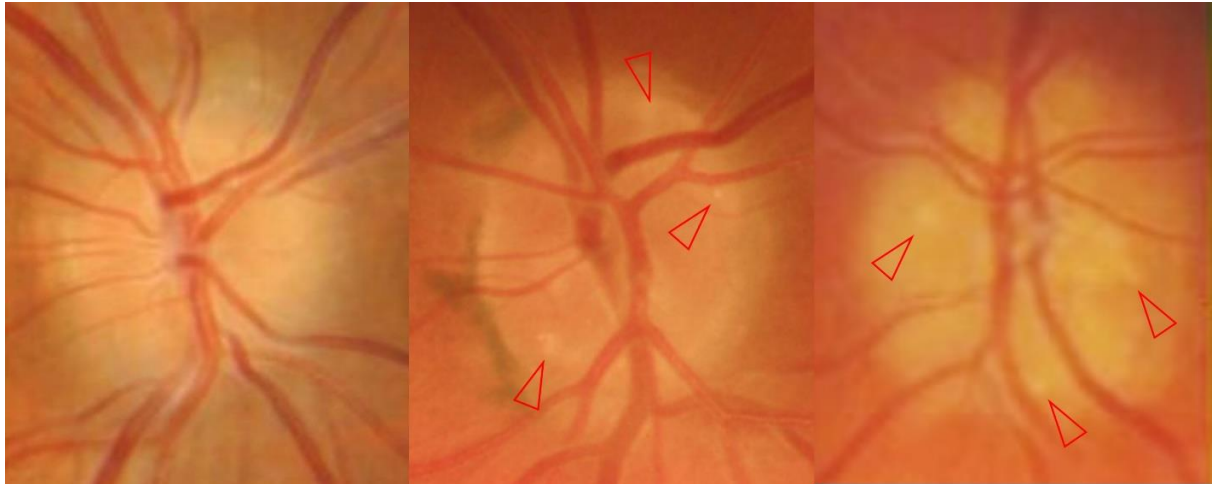
Figure 3: Participants with ONHD, buried or visible.

Images of ONH (left, id nr. 3; middle, id nr. 153; right, id nr. 76) where ONHD shown as bright irregular deposits (red arrowheads). Image to the left have buried ONHD since they are not visible, but are the reason for the swelled appearance, and blurred margins.

1.2.4 Fundus autofluorescence

ONHD are hyperautofluorescent (Hamann et al., 2018) due to their high amount of mitochondria which contain the hyperautofluorescent fluorophore porphyrins (Schmitz-Valckenberg, Holz, Bird, & Spaide, 2008). The porphyrins are used in the respiratory chain in the mitochondria and not normally detected within the optic disc (Partha et al., 2006; Schmitz-Valckenberg et al., 2008), but released into the extracellular space during cell death and degeneration (Nagata, 1997). This supports the mechanism that ONHD is a result of cell death, and that mitochondria are extruded into the extracellular space, there is a continuous calcium deposition leading to increase in size (Sato et al., 2013). Several terms for hyperfluorescence are used in the literature; hyperfluorescence, autofluorescence and hyperautofluorescence, but all describes the same.

The hyperautofluorescence depends on the anatomic location of the ONHD; in studies with visible drusen 93-100% are autofluorescent (Gili, Flores-Rodríguez, Yangüela, & Herreros Fernández, 2013; Pineles & Arnold, 2012), while buried drusen are hyperautofluorescent in 92% of cases (Gili, Flores-Rodríguez, Yangüela, et al., 2013). A lower sensitivity is found when examining children as they are more likely to have non-calcified ONHD. In the cases

with buried ONHD the hyperautofluorescence may be weaker due to the overlying tissue and may therefore be overlooked (Gili, Flores-Rodríguez, Yangüela, et al., 2013; Kurz-Levin & Landau, 1999).

ODE and PHOMS mentioned earlier are on the other hand, not hyperautofluorescent (Malmqvist, Sibony, et al., 2018; Wang et al., 2018).
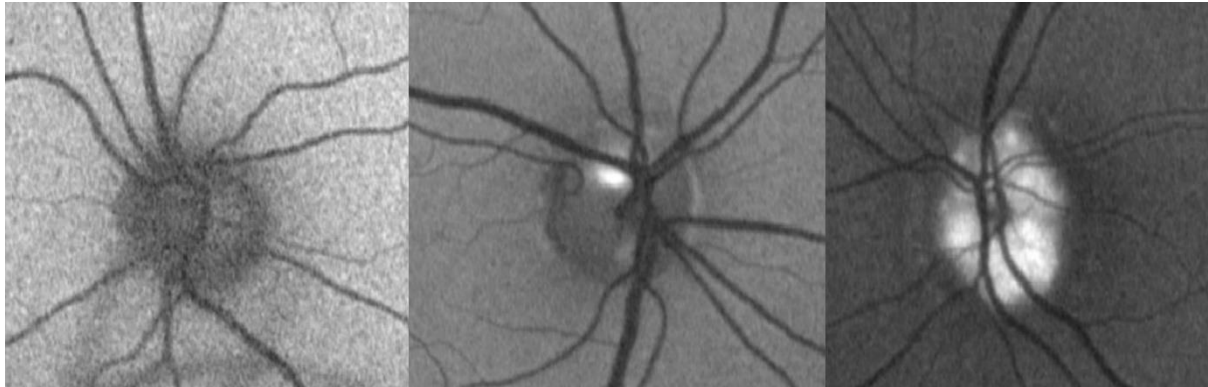

Figure 4: Autofluorescent imaging

AF-images of ONH (id nr. from left to right: 251 OS, 46 OD, 76 OS) with varying degrees of hyperautofluorescence. Left image is an ONH with PHOMS, as described above, with no hyperautofluorescence. Image in the middle shows bright hyperautofluorescence in the mid-periphery at 11 o'clock and dim hyperautofluorescence in inferior part at 6 o'clock which is not so apparent as the superior hyperautofluorescence. Image on the right side shows bright hyperautofluorescence in major part of the optic disc.

1.2.5 B-scan Ultrasound

B-scan ultrasound has previously been the gold standard for detection of ONHD (Kurz-Levin & Landau, 1999). The calcification of the ONHD are detected and they appear as highly reflective round structures that can also be identified with the posterior shadowing (Hamann et al., 2018). However, as mentioned above, some ONHD in children are non-calcified and could therefore be missed with this technique, but detected when the ONHD gets calcified (Chang & Pineles, 2016).

This technique is to the best of my knowledge not common in Norwegian optometric practices, and not used in the present study.

1.3 Complications

There are some complications associated with ONHD such as visual field defects, vascular complications and choroidal neovascular membranes. These complications are not registered in the data collection in this study but emphasize the importance to discover ONHD.

1.3.1 Visual field defects

Visual field defects are reported to be prevalent in 11.2% to 87% of eyes with ONHD, where the latter only consisted of clinically visible ONHD (Hamann et al., 2018; Lorentzen, 1966). It is found that visual field defects are more commonly observed in eyes with visible ONHD (Wilkins & Pomeranz, 2004). However, the severity of the visual field defect depend on the ONHD volume rather than anatomic location (buried or superficial), and since the visible ONHD tend to be larger in volume they will more often lead to RNFL thinning and visual field defects (Malmqvist, Lindberg, et al., 2017; Sato et al., 2013; Skaat et al., 2017).

Different theories for visual field defects have been suggested. The first is that the calcified bodies compress the adjacent ganglion cell axons, leading to ganglion cell death and axonal degeneration (Katz & Pomeranz, 2006; Malmqvist, Lindberg, et al., 2017).The second alternative explanation is due to vascular comprise leading to ischemia within the optic nerve head (Auw-Haedrich et al., 2002). The most common visual field defect in ONHD, are inferonasal and inferotemporal defects, enlargement of the blind spot and a generalized constriction (A. G. Lee & Zimmerman, 2005; Lorentzen, 1966).

ONHD is found to cause not only afferent damage, but also retrobulbar axonal degeneration similar to glaucoma, and could also be viewed as a neurodegenerative disorder (Chan, Morgan, Yu, & Balaratnasingam, 2017).

1.3.2 Vascular complications

Retinal haemorrhages and vascular occlusions are regularly associated with ONHD (Auw-Haedrich et al., 2002; Lam et al., 2008). In most cases haemorrhages do not lead to impaired visual function (Auw-Haedrich et al., 2002). Retinal vascular occlusions and ischemic optic

neuropathy are the only known causes of acute decrease in vision due to ONHD (A. G. Lee & Zimmerman, 2005; Lorentzen, 1966).

Drusen associated ischemic neuropathy (DAION) and non-arthritic ischemic optic neuropathy (NAION) is suggested to have the same pathogenesis of visual loss, and associated with a small scleral canal (Purvin, King, Kawasaki, & Yee, 2004).

Choroidal neovascular membranes are found to be more common in children with ONHD where it is found in 25% of children with ONHD (Duncan, Freedman, & El-Dairi, 2016). To be able to properly detect neovascular membranes, other imaging techniques like OCT angiography, fluorescein angiography or indocyanine green, must be used.

These conditions will not be addressed further in this study.

1.4 Differential diagnoses

1.4.1 Papilledema

As mentioned, ONHD mimic ODE, particularly when buried, and misdiagnosing ONHD as a true disk edema may lead to an invasive and unnecessary treatment and cost (Chang & Pineles, 2016). In a study concerning suspected papilledema in children, 52% were misdiagnosed with ODE and 34.6% of these had ONHD as the last diagnose (Liu et al., 2014).

1.4.2 Glaucoma

When there is coexisting glaucoma together with ONHD, assessment of optic nerve head is difficult as the ONHD obscure the cup and further makes assessment of cup-disc ratio difficult (Yi et al., 2009). However, the visual field defects seen in cases of ONHD are similar to those of glaucoma.

1.5 Treatment

Although there is no established treatment available, a correct diagnosis of ONHD provides prognosis and avoids unnecessary work-up (Lam et al., 2008). Lowering intraocular pressure has been proposed as a neuroprotective treatment in eyes with ONHD, similar to reducing risk of progression in optic nerve damage in patients with glaucoma (Auw-Haedrich et al., 2002; Chang & Pineles, 2016), but in a systematic examination of 236 mainly normotensive eyes

there was no significant association between IOP and visual field defects (Nolan et al., 2017). As stated by Hamann et al. (2018); in eyes with coexisting ocular hypertension and ONHD it is impossible to know if a visual field defect is a caused by the ONHD or the raised intraocular pressure as the two conditions produce quite similar visual field defects (Hamann et al., 2018). In eyes with ONHD where visual field defects are present, regularly tonometry and visual field examinations are suggested as the predamaged nerve fibres may be more sensitive to raised or even normal IOP than normal subjects (Auw-Haedrich et al., 2002).

2 Methods

2.1 Research objectives and significance

The main objective of this study is to investigate the prevalence of optic disc drusen in subjects over the age of 18 visiting an optometric practice in Norway, by means of different imaging techniques; spectral domain optical coherence tomography (SD-OCT), fundus photography and fundus autofluorescence (FAF).

The main objective of this study is based on the following questions:

1. Among persons who undergo a routine optometric examination in an optometric practice in Norway, what proportion of participants have optic nerve head drusen identified by means of SD-OCT, fundus photography and FAF?

2. Are there any difference in the prevalence of subjects with optic nerve head drusen when comparing the different imaging methods; OCT, fundus photo and fundus autofluorescence?

The second objective of the study is to investigate the characteristics of the optic nerve head drusen found in the same population:

The second objective is based on the following research questions:

1. In subjects with optic nerve head drusen identified by means of OCT, what is the mean greatest observed diameter of the ONHD?

2. Measured with SD-OCT, fundus photography and FAF, what is the location of the optic nerve head drusen, and does the ONHD size affect the visibility?

3. Measured with SD-OCT, are there any differences in RNFL-thicknesses in subjects with optic nerve head drusen compared to the normal subjects, and are there any differences in RNFL thickness when comparing the visibility of the ONHD?

4. In eyes with ONHD, do the ONHD diameter and the number of ONHD affect the RNFL thickness?

5. In subjects with optic nerve head drusen, are there any difference in the disc diameter measured with SD-OCT compared to disc diameter in normal subjects?

The study will give knowledge about the prevalence of ONHD in a Norwegian population that are visiting an optometric practice. OCT is increasingly used among Norwegian optometrists,

and knowledge about the prevalence and characteristics of both visible and buried ONHD with different methods are of importance in the assessment of atypical optic nerve heads and may further improve clinical procedures and guidelines for Norwegian optometrists.

Similar studies have not been performed in Norway earlier.

2.2 Study design

The study has a cross sectional study design, and the target population was men and women above the age of 18 who went through an optometric eye examination in Norway. Eligible participants in the study are males and females between 18 and 100 years who went through a routine optometric examination at Krogh Optikk Majorstuen between 6th of November 2018 and 6th January 2020.

2.3 Patient selection

2.3.1 Recruitment

Recruitment of subjects took place at Krogh Optikk Majorstuen in Oslo in the period from 6th of November 2018 to 6th of January 2020. Patients who came for an optometric examination was invited to participate in the study and was given oral and written information about the study together with consent form. If the patient gave his/her written consent, the relevant data was transferred to a dedicated registration form. Recruited patients' names were replaced with an id-number (1,2, 3….) to ensure anonymity of the participants. The list that links subjects' name and id-numbers will be deleted at the end of the study. The study aimed for 385 participants to give information about prevalence of optic disc drusen in a Norwegian population. Number of participants was calculated using formula for calculating sample size (Daniel, 1999). The following values was put in the equation; prevalence (P) 50% when a low prevalence is expected or if the prevalence is unknown, Z= Z statistic for a level of confidence= 1.96 for a level of confidence of 95% and precision (d)= 5%.

$$n = \frac{Z^2 \cdot P(1-P)}{d^2} = \frac{1{,}96^2 \cdot 0{,}5(1-0{,}5)}{0{,}05^2} = 384{,}2 \approx 385$$

The required number of participants was 385

2.3.2 Exclusion criteria

Subjects were excluded if the image quality was not good enough.

- If the images had insufficient quality; new photos were taken if image quality<30. The value is an indication from the IMAGEnet i-base software. If persisted quality <30, the patient was excluded.
- If any corneal or lens opacities blurred either fundus photography or AF-image with optomap – resulting in dark images.
- Poor image quality due to small pupils, poor wetting of the corneal surface, blinking or excessive eye movements.

Table 1: Grading scale for exclusion/inclusion in study.

	Image quality OCT	Exposure fundus photo	Autofluorescence
YES Good quality	Image quality>30 Clear structure, whole scan, no lacking information due to blink or poor wetting of cornea	Even exposure	Clear structures, easy to distinguish optic nerve head from surrounding structures.
NO Poor quality	Image quality<30, blurred structures, lacking information due to blink or poor wetting of cornea	Obvious under/over exposure	Blurred structures, Difficult to distinguish optic nerve head from surrounding structures.

2.4 Data acquisition

All subjects went through a standard optometric examination of both eyes in agreement with the clinical guidelines of the Norwegian Association of Optometry. This included history taking of medical and ocular health, visual acuity measurement (Snellen), binocular vision assessment, refraction, posterior and anterior segment biomicroscopy, pupil measurement, measurement of intraocular pressure and fundus photography. These tests are performed with standard optometric equipment commonly used in an optometric clinic. Experienced authorized optometrists performed all data collection, tests, and procedures.

The results from the standard optometric examination was registered in the clinic's patient journal system (Headsoptics). Data obtained from the Optomap, OCT and fundus camera was stored in the dedicated software within the instruments.

The anonymized data collected for both eyes were transferred to a registration form in Excel (Microsoft). This included refraction (spherical equivalent), sex, visual acuity, vertical disc diameter, ONHD visibility with fundus image, number of drusen, RNFL thickness, size of ONHD, autofluorescence of ONH. Missing values was registered as "9999". Pupil dilation (with Tropicamide 0.5%) was done when needed to obtain adequate image quality.

A Spectral-Domain Optical Coherence Tomograph (SD-OCT) from Topcon (Japan) called 3D OCT-1 Maestro, that combines OCT and fundus image was used. It captures 50 000 A-scans per second (Medical, 2016). The following scanning procedure was used: Disc scan with 128 scans in a 6x6mm cube (1 frame per section) and a radial scan with 12 sections of 6 mm, 4 frames per section. Both scans included a colour fundus image. Both scan patterns were centred on the ONH.

The autofluorescent images were obtained with Optomap Daytona and utilizes a green laser with a wavelength of 532 nm (Browning, 2013).

2.5 Data analysis

All images were analysed by the project manager who is an experienced optometrist. The software of Topcon 3D OCT-1 Maestro (IMAGEnet i-base, version 6) was used to assess all OCT parameters. The data were analysed in this specific order; (1) ONHD visibility on fundus image, (2) RNFL thickness, (3) number of ONHD, (4) diameter of largest observed ONHD (5) disc diameter, (6) ONHD visibility, Autofluorescence on Optomap.

1) ONHD visibility on fundus image: Defined as bright yellow, irregular deposits within the optic nerve head. Registered as present or not (yes or no) in the superior, nasal, inferior and temporal quadrant of the optic nerve head.
2) RNFL thickness: Defined as the thickness (µm) of the peripapillary retinal nerve fiber layer (RNFL) in the superior, nasal, inferior and temporal quadrant of the optic nerve head, measured with volume scan of the disc. The global RNFL thickness was also registered.

3) Number of ONHD: The ONHD using OCT was defined as a mass with hyporeflective core with full or partial hyperreflective margins mainly located anterior to the lamina cribrosa (Merchant et al., 2013; Sato et al., 2013; Slotnick & Sherman, 2012). Number registered in the superior, nasal, inferior and temporal quadrant of the optic nerve head. Total quantity was divided into groups where "few ONHD" = $>0\leq3$, "many ONHD" = >3).

4) Diameter of largest observed ONHD: The largest observed diameter (µm) of all ONHD was measured on the radial scan with the integrated caliper tool, as illustrated in Figure 5.

Divided into groups where "small ONHD" = diameter $>0\leq310$ µm, "large ONHD" = diameter>310µm for right eyes and "small ONHD=diameter $>0\leq221$ and "large ONHD" diameter>221µm for left eyes.
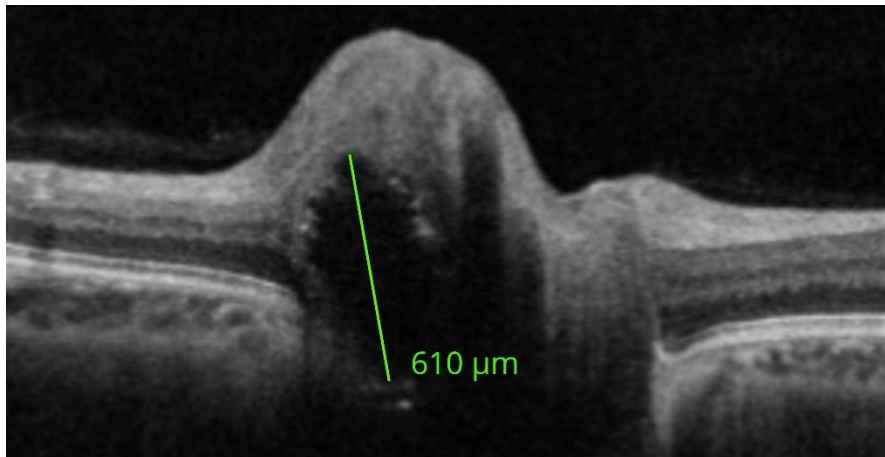

Figure 5: Measurement of largest observed ONHD diameter.

5) Disc diameter: Defined as the vertical opening in Bruch's membrane bordering the optic disc (Bellezza et al., 2003). The disc diameter (µm) was measured on the vertical section in the radial scan by using the integrated caliper tool, illustrated in Figure 6.

6) Visibility of ONHD with Autofluorescence measured with Optomap: Defined as hyperfluorescent parts of the optic nerve head, registered as present or not (yes or no) in the superior, nasal, inferior and temporal quadrant of the optic nerve head.
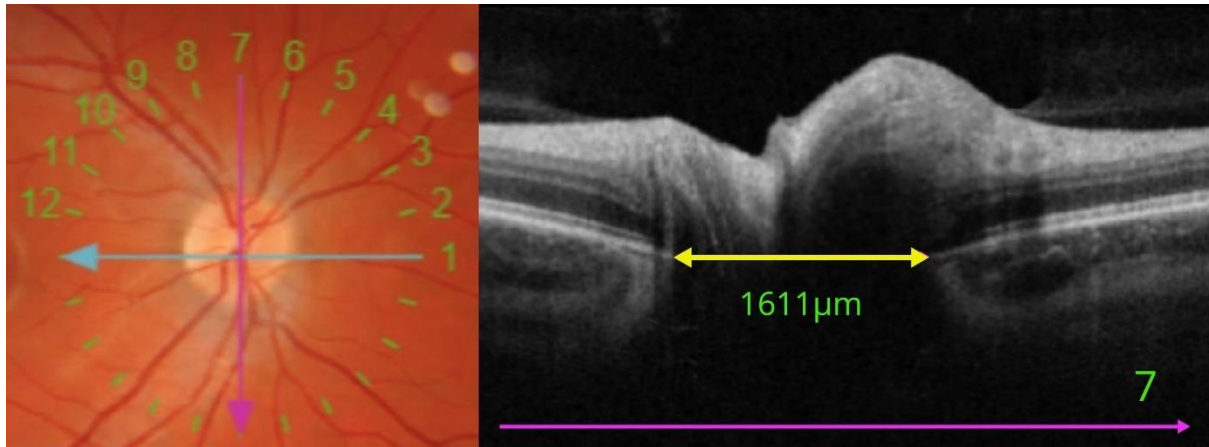
Figure 6: Measurement of vertical disc diameter.

Left image shows a radial scan centered on ONH (right eye, id nr. 74). Right image shows an OCT-scan of the vertical (purple) line with measurement of vertical diameter (yellow arrow) by using the caliper tool integrated in the OCT-software.

One person with a ph.d. in retinal imaging (principal investigator) and one ophthalmologist was available for analyzing images if the project manager was unsure of the diagnosis. Both are employed at the University of Southeastern Norway.

2.6 Statistical analysis

The statistical analysis was performed in IBM SPSS Statistics 24. The excel-sheet was quality-checked and transferred to SPSS. The missing data registered as 9999 in Excel was excluded and registered as "missing"-data in SPSS.

Descriptive statistics was used for calculating prevalence, means and standard deviations.

Cohen's Kappa (κ) statistic was used to determine interrater reliability between categorical variables; values of 0.81-1.0 indicates an almost perfect agreement; 0.61-0.80, substantial agreement; 0.41-0.60, moderate agreement; 0.21-0.40, fair agreement; 0.0-0.20, slight agreement; ≤ 0, poor agreement (Landis & Koch, 1977).

Correlation analysis was calculated using Welch's ANOVA when comparing more than two groups. The method was chosen when the variances and sample sizes were unequal.

between more than two groups. Independent Samples T-Test were used to compare means between two groups.

2.7 Ethical considerations

This master thesis was approved by the Regional Committee for Medical Research Ethics for the Southern Norway Regional Health Authority (REK), REK 2018/1656 "Forekomst av optisk disk druser i en norsk optometrisk praksis". All participants included in the study went through a standard optometric examination that follows the clinical guidelines of Norwegian Association of Optometry. All procedures were non-invasive and did not cause any pain or severe discomfort for the patient. A written informed consent was signed before including the subject in the study. All participants were informed that they at any time could withdraw from the examinations. The files containing patient information will be deleted when the study ends, at latest 15th June 2020.

All personal information and data of the participants in the study were handled confidentially. Personal information and results from the standard examination including retinal images and scans were saved in the clinic's dedicated systems according to present laws of personal information and confidentiality. Information related to the study was unidentifiable and saved externally. The saved information for each participant was sex, age, refraction, diseases, ocular health, and medical use in addition to the retinal images and scans. The list that links patients' name and id-numbers will be stored responsibly for a limited period and deleted in the end of the study.

The project follows the General Data Protection Regulation article 6a and article 9 nr.2 and the participants consent.

Tropicamide (0.5%) was used for dilation if the pupil size (< 2.5 mm) restricts the image quality. The subjects who were dilated was given oral information of the possible side effects that might occur following the use of Tropicamide drops. The side effects might be a slightly burning sensation immediately after installation of the drops which lasts for approximately 10-20 seconds. They could also notice an increased sensitivity to light as the pupil aperture is larger after dilation. Before dilation, the anterior chamber angle was measured by slit lamp examination and graded by the Van Herick scale. Subjects with a Van Herick grade < 2 was

not dilated due to the slight risk for acute angle closure glaucoma. The subjects were asked if they had experienced any reactions to drugs or if they had any allergies.

The Spectral-Domain OCT with fundus camera and Optomap are both non-mydriatic and non-invasive. Both SD-OCT and Optomap utilize laser in Laser Class 1, which is approved as safe where neither the direct, scattered nor reflected laser beam produce any risk or injuries (TNRPA, 2012). These two instruments are not associated with any discomfort. Optomap was included in the standard examination as well as OCT macula scan and disc scan. The additional radial scan with OCT needed for the study took approximately 2 minutes extra for each participant.

The participants were followed up or referred to a specialist if there were any special findings that needed referral, including suspected papilledema. The subjects with ONHD were referred if findings included haemorrhages, other vascular complications, or visual field defects.

3 Results

A total of 305 subjects was included in the study with 187 (61.3%) females and 118 (38.7%) males. The subjects' age ranged from 19-82 years where mean age was 45.41 ($\pm$ SD 14.73) years. Mean refractive error measured as spherical equivalent was -1.1 $\pm$2.8 D for both right and left eyes. The mean disc diameter was 1598.5 ($\pm$196.9) µm for right eyes and 1622.8($\pm$191.1) µm for left eyes.

Three of the 305 participants (0.98%) had a glaucoma diagnose in this study. One subject (0.3%) was referred to an ophthalmologist who confirmed a diagnosis of papilledema. These 4 participants were excluded in RNFL analysis.

3.1 Prevalence

3.1.1 Prevalence OCT

Participants with ONHD identified with SD-OCT, had a mean age of 41.78 years (SD $\pm$12.87) ranging from 24 to 68 years. A total of 23 participants were identified with ONHD with OCT where 16 (69.6%) were female and 7 (30.4%) were male. This gives a prevalence of 23/305=0.075≈7.5% [CI 4.8-11%]. ONHD were bilateral in 60.9% of these cases. Of all participants included in the study, 19 (6.2%) had ONHD in the right eye [CI 3.8-9.6%], 18 (5.9%) had ONHD in the left eye [CI 3.5-9.2%], (Figure 7) and a total of 37/610 (6.1%) eyes had ONHD identified with OCT. Table 2 shows a summary for all the measured prevalence.

3.1.2 Prevalence Photo

Participants with ONHD identified with fundus photography, visible ONHD, had a mean age of 45.90 years (SD $\pm$10.97) ranging from 29 to 56 years. A total of 10 participants had visible ONHD where 8 (80%) were female and 2 (20%) were male, resulting in a prevalence of 10/305=0.033≈3.3% [CI 1.6-5.9%]. ONHD were bilateral in 40% of cases. Of all participants, 6 (2%) had ONHD in the right eye [CI 0.7-4.2%], 8 (2.6%) had ONHD in the left eye [CI 1.1-5.1%] and a total of 14/610 (2.3%) eyes had ONHD identified with fundus photography.

3.1.3 Prevalence AF

Participants with ONHD identified with AF had a mean age of 41.1 years (SD ±12.72) ranging from 24 to 68 years. ONHD was identified in a total of 22 participants where 16 (72.7%) were female and 6 (27.3%) were male. This results in a prevalence of 22/305=0.069≈7.2% [CI 4.6-10.7%]. ONHD were bilateral in 40.9% of cases. Of all the participants 17 (5.6%) had ONHD in the right eye [CI 3.3-8.8%], 14 (4.6%) had ONHD in the left eye [CI 2.5-7.6%] and a total of 31/608 (5.1%) eyes had ONHD identified with autofluorescence.

Table 2: Summary of group demographics, n=305.

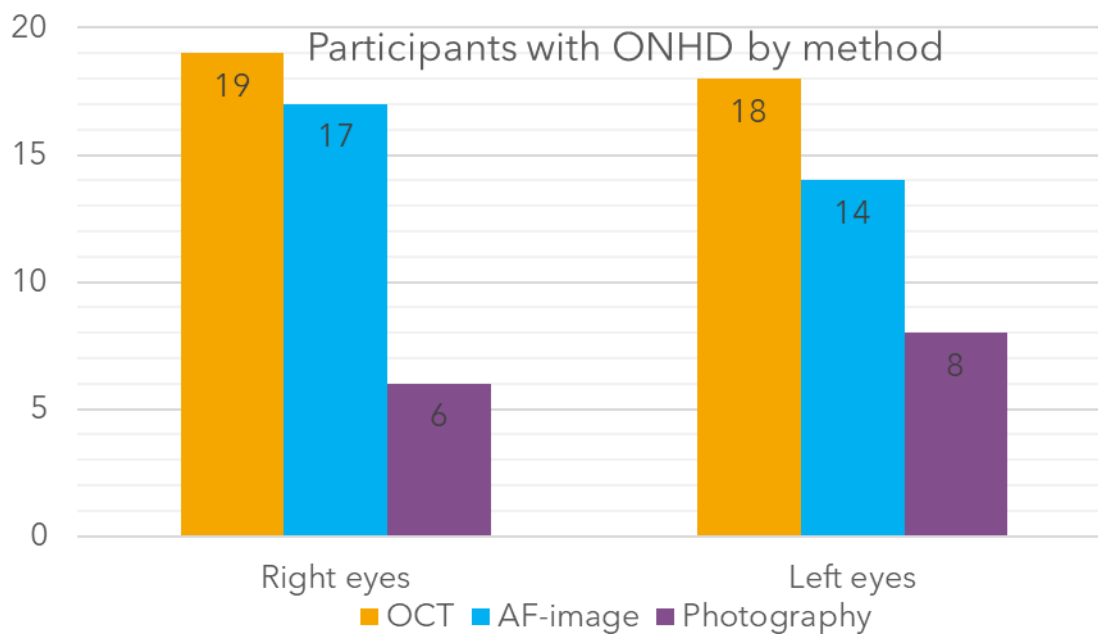|	Prevalence	Mean age (±SD)	Female / male	ONHD 1 eye	ONHD both eyes
OCT	n=23 7.5% [CI = 4.8-11%]	41.8 (±12.87)	16(69.6%) / 7(30.4%)	9 (39.1%)	14 (60.9%)
Photo	n=10 3.3% [CI 1.6-5.9%]	45.9 (±10.97)	8 (80%) / 2 (20%)	6 (60%)	4 (40%)
AF	n=22 7.2% [CI 4.6-10.7%]	41.1 (±12.72)	16 (72.7%)/ 6 (27.3%)	13 (59.1%)	9 (40.9%)

Figure 7: Number of participants with ONHD by detection method.

Table 3 shows a comparison of the mean age between the subjects with no ONHD, buried drusen (detected with OCT, but not visible on fundus photography) and visible drusen (visible on fundus photography). Analysis shows that there was no significant difference in age between these groups.

Table 3: Mean age in the different groups.

Buried ONHD are detected with OCT, but not with photography. Visible ONHD are only detected with photography.

Mean age (years)	Right eyes (±SD)	Left eyes (±SD)
No ONHD	45.7 (±14.9) *n=286*	45.6 (±14.8) *n=287*
Buried ONHD	38.6 (±10.8) *n=13*	40.6 (±15.9) *n=10*
Visible ONHD	46.50 (±11.4) *n=6*	46.50 (±10.4) *n=8*

No significant difference in age between subjects with buried ONHD and visible ONHD (p=0.164 for right eyes and p=0.380 for left eyes).
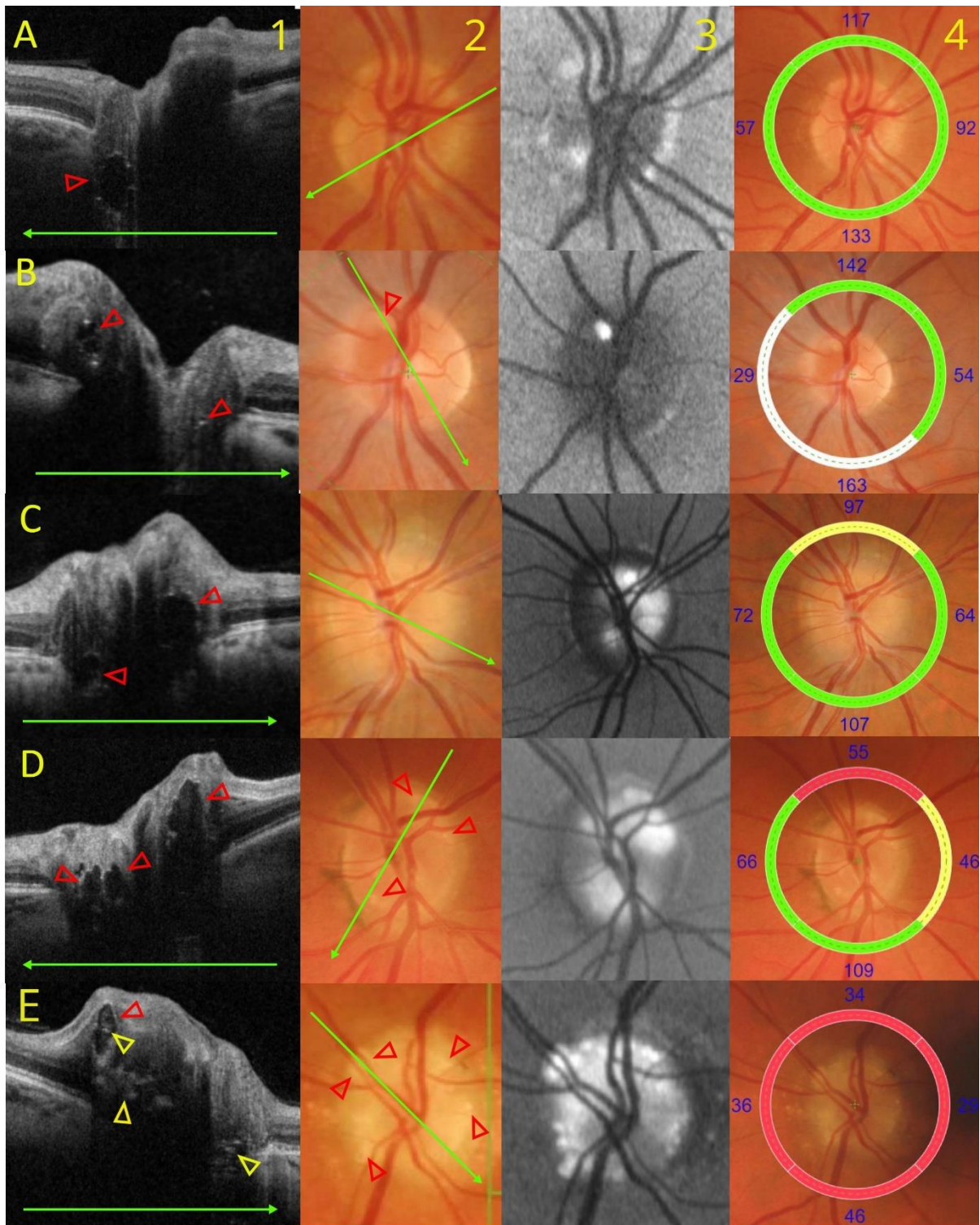
Figure 8: Illustration of ONH with ONHD with multimodal imaging.

The rows A-E are images of ONH from some of the ONHD subjects collected in our study. Column 1 shows OCT-scans where green line indicates the direction of the scan. ONHD are marked with red arrowheads on OCT-scans (1), and fundus image (2) (when visible). Hyperreflective foci and conglomerates are marked with yellow arrowheads. The AF-images

*(3) shows varying hyperautofluorescence. Fundus photo with RNFL (4) in superior, nasal, inferior and temporal quadrant with either white, green, yellow or red colour indicates RNFL thickness above, within, outside 5% or outside 1% of the normal limbit, respectively. The fundus photos (2) are marked with a green line that illustrates the OCT-scan line. **A** (right eye, id nr.167), have an ONHD detected on OCT (red arrowhead) and AF-image where it shows dim hyperfluorescence. No apparent ONHD visible on fundus photography. **B** (left eye, id nr.289), where 2 ONHD are located closely (left side of OCT-scan) which correspond with bright deposit located at 11 o'clock on fundus photography and the hyperfluorescent part on the AF-image. The small ONHD located on the right side, posterior to Bruchs membrane is not visible on fundus photography or AF-image but the disc margin is blurred from 9-12 o'clock. **C** (right eye, id nr.3), where OCT scan shows 2 ONHD on either side of Bruchs membrane, where the one above has an indistinct posterior margin, but there is some hyperreflectivity deeper in the ONH. Fundus image shows blurred margins, but no apparent ONHD are visible in the surface. AF-image show hyperfluorescence mainly from 10-8 o'clock. The RNFL is thinner in the superior quadrant, outside 5% of the normal limit of the normative database. **D** (right eye, id.n r 153), has several ONHD detected with OCT. Some are also visible on the fundus image. AF-image show hyperfluorescence from 10-3 o'clock and 5-8 o'clock. The RNFL is thinner in the superior and nasal quadrant, outside 1% and outside 5% of the normal limit. **E** (left eye, id nr.35) has the most apparent visible ONHD and as we see from the OCT-scan there are these small hyperreflective conglomerates. On the AF-image the whole ONH is hyperfluorescent apart from a small sector from 5-6 o'clock which is where the small conglomerates are seen on the OCT-scan. The RNFL is thinner in all quadrant, outside 1% of the normal limit.*

3.1.4 Difference between methods

To evaluate the correlation between the different methods, an interrater reliability analysis was used called Cohen's Kappa (κ). In other words, how well do the different imaging methods detect ONHD.

Right eye: Comparing OCT with fundus photography gave a Kappa value of 0.464 and a sensitivity of 31.6%. Since the Kappa value is between 0.41 and 0.60 it is considered as a moderate agreement between the two methods. Comparing OCT with AF gave a Kappa value

of 0.94 and a sensitivity of 89.5%. The Kappa value is between 0.81 and 0.99 it is considered as an almost perfect agreement between the two methods.

Left eye: Comparing OCT with fundus photography gave a Kappa value of 0.601 and sensitivity of 44.4%. Since the Kappa value is between 0.41 and 0.60 it is considered as a moderate agreement between the two methods. Comparing OCT with AF gave a Kappa value of 0.87 and a sensitivity of 77.8%. The Kappa value is between 0.81 and 0.99, also for this eye it is considered as an almost perfect agreement between the two methods. Table 4.

Table 4: Correlation of imaging techniques.

Correlation	RIGHT EYE	LEFT EYE
OCT vs AF	Kappa: 0.94 ⇒ almost perfect agreement Sensitivity: 89.5%	Kappa: 0.87 ⇒ almost perfect agreement Sensitivity: 77.8%
OCT vs fundus	Kappa: 0.464 ⇒ moderate agreement Sensitivity: 31.6%	Kappa: 0.601 ⇒ moderate agreement Sensitivity: 44.4%
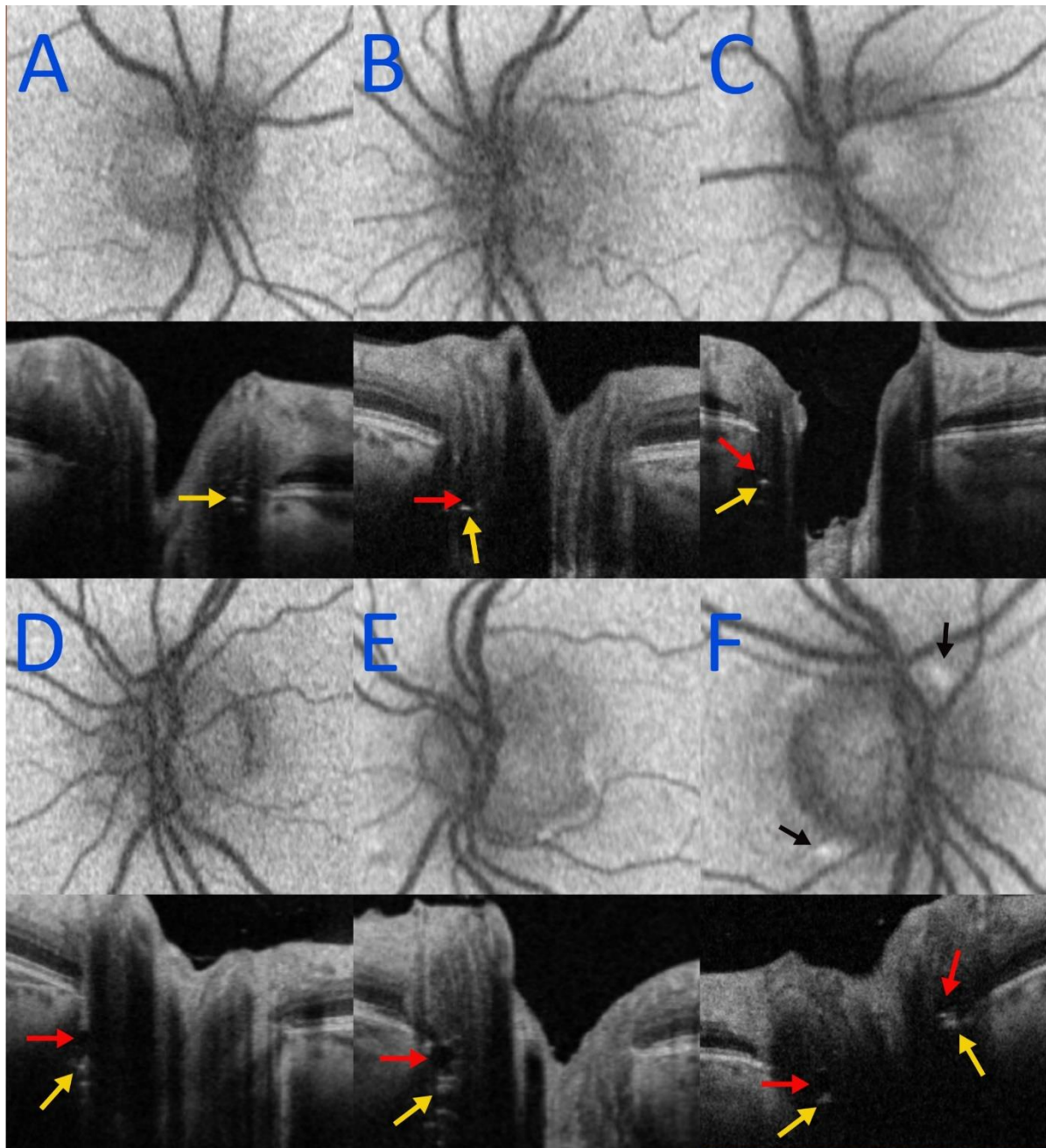
Figure 9: The ONHD that were detected with OCT but did not show hyperautofluorescence.

A-F show AF-image with the belonging OCT-scan below. ONHD shows as hyporeflective mass (red arrow), hyperreflective foci and lines (yellow arrows). The peripapillary hyperautofluorescence in F (black arrows) does not correspond with the location of the ONHD detected in the OCT-scan.

3.2 ONHD diameter

The ONHD size registered in this study is the largest observed ONHD diameter in each eye for each participant with ONHD identified with OCT. Largest ONHD diameter in right eyes had a range from 72um to 462 um and a mean of 267.42 ($\pm$123.3) µm [CI 207.97-326.87]. Largest ONHD diameter in left eyes had a range from 40um to 610 um and a mean of 244.78 ($\pm$172.2) um [CI 159.16-330.40].

The ONHD that were visible with fundus photography had a mean diameter of 294.3 ($\pm$83.0) [CI 207.2-381.5] µm for right eyes and 334.4 ($\pm$158.4) [CI 201.7-466.55] µm for left eyes measured with OCT. This was significantly larger ($p<0.05$) than the ONHD that were not detected on fundus images, with an ONHD diameter of 255($\pm$139.3) [CI 170.8-339.2] µm and 173.3 ($\pm$154.0) [CI 63.2-283.5] for right and left eyes respectively (see table 5 and figure 10). The ONHD that did not show hyperautofluorescence on the AF-image (Figure 9) had a mean diameter of 86($\pm$19.8) [CI -9.2-68.4] um for right eyes and 82.0 ($\pm$34.1) [CI 27.7-136.3] um for left eyes. The ONHD that showed hyperautofluorescence on the AF-image had a larger mean diameter than the ONHD with no hyperautofluoresence; 288.8 ($\pm$111.8) [CI 220.6-443.1] um for right eyes ($p<0.023$) and 291.3 ($\pm$167.4) [CI 194.6-387.9] um for left eyes ($p<0.001$), (Table 5 and figure 11).

Table 5: ONHD diameter by detection method.

Summary of mean of the greatest ONHD diameter detected by different imaging methods divided in groups.

Mean diameter of greatest ONHD (μm)	Right eyes (±SD)	Left eyes (±SD)	P-value
OCT	267.4 (±123.3) n=19	244.78 (±172.2) n=18	
No AF, only detected with OCT	86.0 (±19.8) n=2	82.0 (±34.1) n=4	RE: p<0.023 LE: p<0.001
AF	288.8 (±111.8) n=17	291.3 (±167.4) n=14	
Buried ONHD	255(±139.3) n=13	173.3 (±154.0) n=10	OU: p<0.05
Clinically visible ONHD, photo	294.3 (±83.0) n=6	334.4 (±158.4) n=8	

P-value calculated with Student T-Test
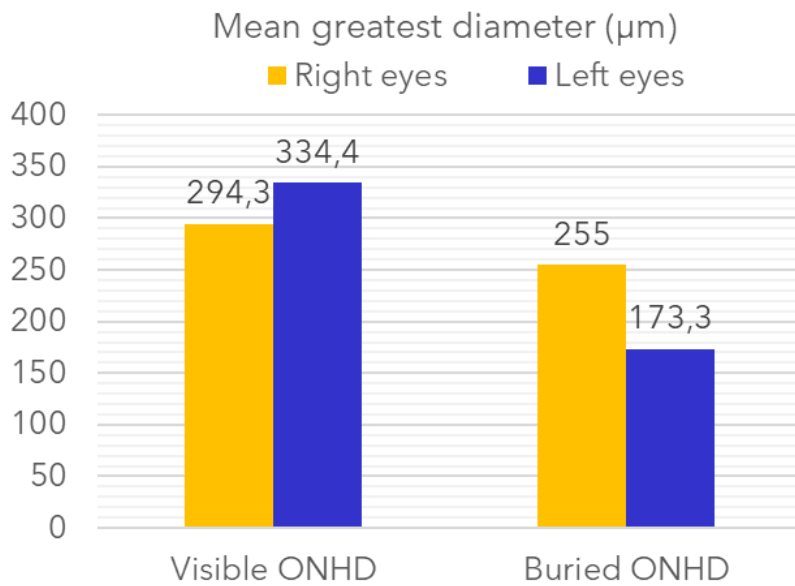
Figure 10: ONHD diameter by visibility on fundus photography.

Graph shows the mean diameter of the largest detected ONHD, sorted by visibility on photography. The buried ONHD were visible on OCT, but not on photography.
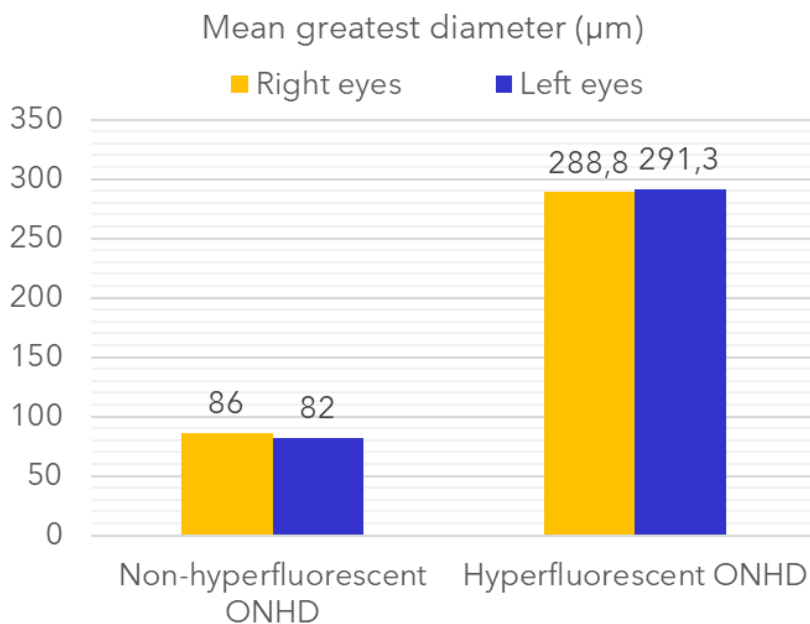
Figure 11: ONHD diameter by visibility on AF-image.

Graph shows the mean diameter of the largest detected ONHD, sorted by visibility on AF-image. Hyperfluorescent ONHD and those only detected with OCT (non-hyperfluorescent ONHD).
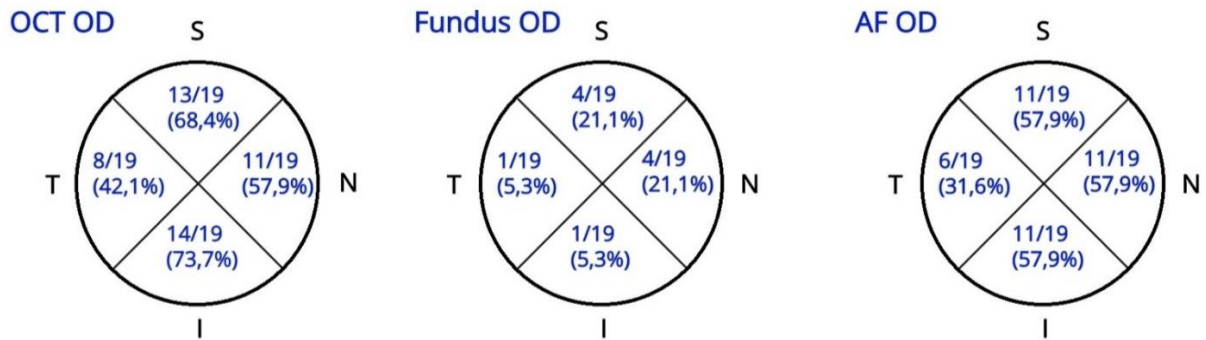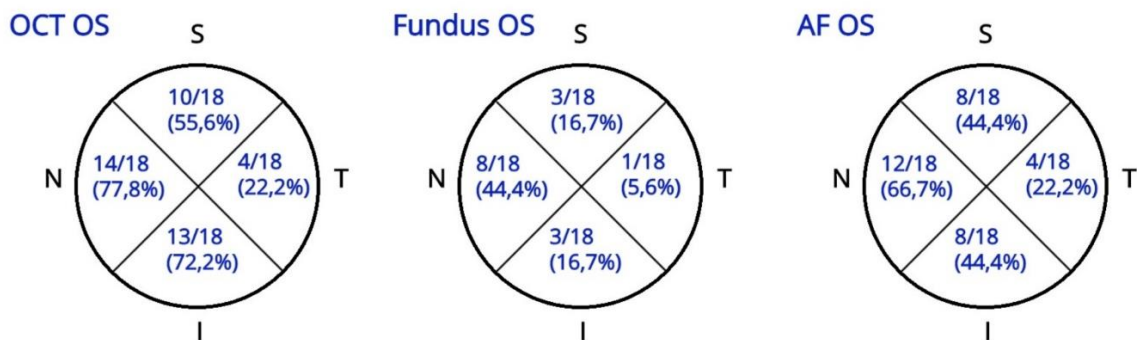
3.3 Location of ONHD

Figure 12: Location of ONHD, right eyes.

The location is presented as a percentage of presence in the sectors of the ONH in right eyes compared to the total number of subjects (n=19) with ONHD detected with OCT. Superior (S), Nasal (N), Inferior (I), Temporal (T).

A total of 19 subjects had ONHD in the right eye detected with OCT. In right eyes with ONHD, the percentage of presence with OCT was inferior (73.7%), superior (68.4%), nasal (57.9%) and temporal (42.1%). With fundus photo; superior and nasal (21.1%), inferior and temporal (5.3%). With AF; superior, nasal and inferior (57.9%) and temporal (31.6%). Illustrated in Figure 12.

Figure 13: Location of ONHD, left eyes.

The location is presented as a percentage of presence of ONHD in the sectors of the ONH in left eyes compared to the total number of subjects (n=18) with ONHD detected with OCT. Superior (S), Nasal (N), Inferior (I), Temporal (T).

In left eyes with ONHD, the percentage of presence with OCT was nasal (77.8%), inferior (72.2%), superior (55.6%), and temporal (22.2%). With fundus; nasal (44.4%), superior and inferior (16.7%) and temporal (5.6%). With AF; nasal (66.7%), superior and inferior (44.4%) and temporal (22.2%). Illustrated in Figure 13. Figure 12 and 13 indicate that for both right and left eye the temporal sector is the quadrant with least frequent ONHD, regardless which imaging method used.

3.4 ONHD effect on RNFL

When comparing the RNFL thicknesses between subjects with and without ONHD there was a trend towards reduction of RNFL thickness in the subjects with ONHD compared to normal group (Right eyes: $p = 0.051$, Left eyes: $p = 0.075$), Table 6.

Partial ETA squared (effect size) of 0.055 and 0.037 right and left eyes respectively, means that 5.5 % and 3.7% of the variability in global RNFL is accounted for by the group membership. ONHD is therefore considered to have a small effect on RNFL.

Table 6: Summary of mean global RNLF thickness by the presence of ONHD.

"No ONHD" is participants with no ONHD detected with any method, the normal group. "ONHD" is participants with detected ONHD with OCT. Data presented as mean ±SD. Missing global RNFL thickness for one subject with ONHD.

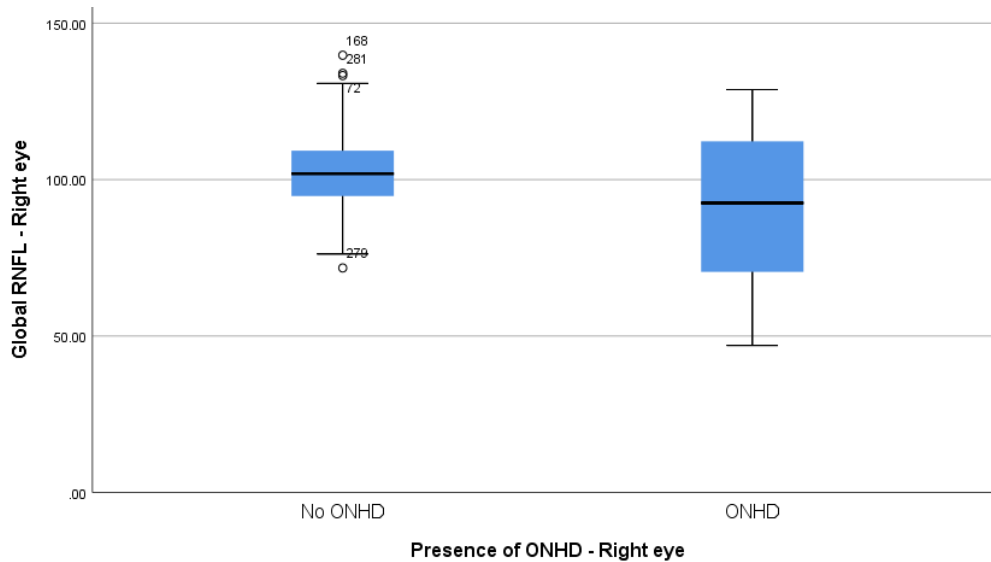|		NO ONHD	ONHD	p-value
Mean global RNFL (μm)	Right eyes	102.2 (±11.0) n=276	89.9 (±24.7) n=18	p<0.051
	Left eyes	102.0 (±11.1) n=276	91.9 (±21.6) n=17	p<0.075

P-value calculated with Student T-Test.

Figure 14: Global RNFL thickness (μm) by the presence of ONHD right eyes.

No ONHD (n=276) and presence of ONHD (n=18). The mean global RNFL thickness is lower for the ONHD group compared to the normal group. The difference is almost significant (p<0.051), which indicates a trend towards thinner RNFL. Global RNFL thickness was missing for one participant with ONHD.
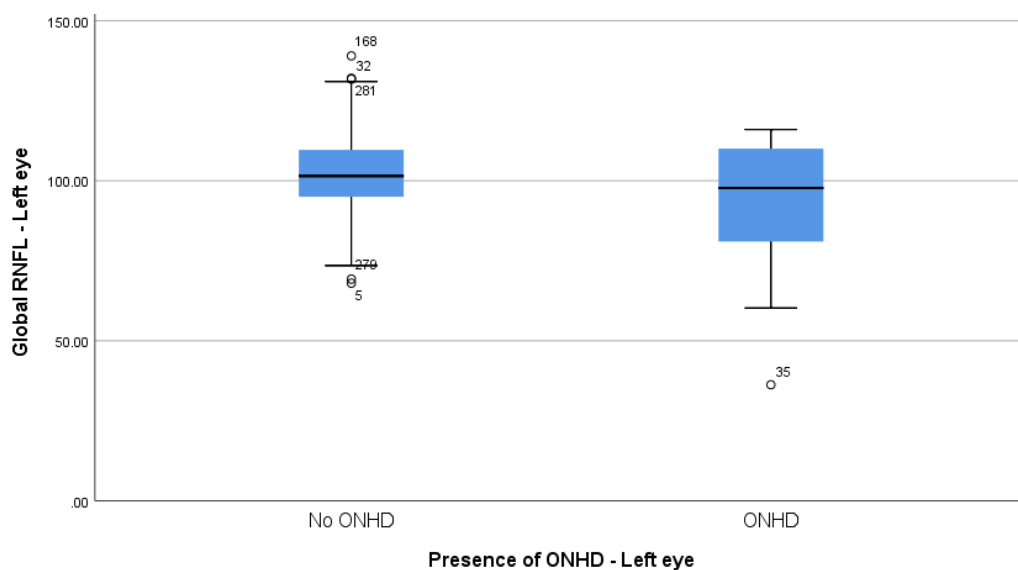

Figure 15: Global RNFL thickness (μm) by the presence of ONHD left eyes.

No ONHD (n=276) and presence of ONHD (n=17). The mean global RNFL thickness is lower for the ONHD group compared to the normal group, but the difference was not significant (p<0.075). Global RNFL thickness was missing for one participant with ONHD.

ONHD subjects with visible ONHD had a mean global RNFL of 70.6 (±17.0) µm for right eyes and 81.4 (±22.2) µm for left eyes. ONHD subjects with buried ONHD had a thicker mean global RNFL of 99.6(±22.4) µm for right eyes and 101.3(±17.2) µm for left eyes. The difference is significant (p<0.013) for right eyes, but only trending towards significant (p<0.056) for left eyes, Table 7.

Comparing the global RNFL between ONHD subjects by detection with AF-image (Table 8), the ONHD subjects with no hyperfluorescence had a mean global RNFL of 117.5 µm (n=1) for right eyes and 110.8 (±3.7) µm for left eyes. The ONHD subjects with hyperfluorescence had a mean global RNFL of 88.3 (±24.4) µm for right eyes and 81.4 (±22.2) µm for left eyes. The global RNFL were significantly thinner for left eyes with hyperautofluorescent ONHD compared to those with no hyperautofluorescence (p<0.002).

For right eyes, the number of participants with ONHD, valid RNFL measurement and no hyperautofluorescence was only 1 – and resulted in a non-significant (p<0.26) difference between the two groups.

Table 7: Visible vs buried ONHD

Mean global RNFL thickness in participants with ONHD detected with OCT, divided into groups by visibility on fundus photo. Measurement of global RNFL was missing for 1 participant.

Mean global RNFL (µm)	Buried ONHD (±SD)	Visible ONHD, photo (±SD)	p-value
Right eyes **n=18**	99.6±22.4 n=12	70.6±17.0 n=6	p<0.013
Left eyes **n=17**	101.3±17.2 n=9	81.4±22.2 n=8	p<0.056

P-value calculated with Student T-Test.

Table 8: Non-hyperautofluorescent vs hyperautofluorescent ONHD.

Mean global RNFL thickness in participants with ONHD detected with OCT, divided into groups by detection with AF-image. Missing global RNFL for one participant.

Mean global RNFL (μm)	NO AF, ONHD (±SD)	AF (±SD)	p-value
Right eyes **n=18**	117.5 n=1	88.3±24.4 n=17	p<0.26
Left eyes **n=17**	110.8±3.7 n=4	86.1±21.6 n=13	p<0.002

P-value calculated with Student T-Test.

If we compare the RNFL thickness by hyperautofluorescence on AF-image, the eyes with hyperautofluorescence had a significantly thinner RNFL than eyes with no hyperautofluorescence (p<0.032 and p<0.021 for RE and LE respectively), Table 9. The group with no hyperautofluorescence here includes subjects without ONHD and subjects with small ONHD only detected with OCT.

Table 9: Hyperautofluorescence

Mean global RNFL divided into groups by hyperfluorescence on AF-image in the whole study sample.

Mean global RNFL (μm)	NO AF (±SD)	AF (±SD)	p-value
Right eyes **n=297**	102.3±11.7 n=280	88.3±24.4 n=17	p<0.032
Left eyes **n=297**	102.0±11.9 n=284	86.1±21.6 n=13	p<0.021

P-value calculated with Student T-Test.

If we compare RNFL thickness based on the ONHD visibility on fundus photography, the eyes with visible ONHD had a significantly thinner RNFL than eyes with no visible ONHD (p<0.006 and p<0.035 for RE and LE respectively), Table 10.

Table 10: Visibility on fundus photography

Mean global RNFL divided into groups by visibility on fundus photography in the whole study sample. The group with no visible ONHD includes normal eyes.

Mean global RNFL (μm)	No visible ONHD (±SD)	Visible ONHD (±SD)	p-value
Right eyes **n=298**	102.1±12.3 n=292	70.6±17.0 n=6	p<0.006
Left eyes **n=297**	101.9±12.1 n=289	81.4±22.2 n=8	p<0.035

P-value calculated with Student T-Test.

3.5 Diameter of ONHD's effect on RNFL

When comparing the RNFL thicknesses between subjects without ONHD, there was a trend towards decreased RNFL with increasing ONHD diameter, but the difference was not statistically significant (Right eyes: $p=0.180$, Left eyes: $p=0.119$) see Table 11. From the graphs below (Figure. 16, 17, 18, 19) there is a declining trend with increasing ONHD diameter. The diameter values were divided into groups based on percentiles; small ONHD (diameter >0≤310 μm) and large ONHD (diameter>310μm), for right eyes; and small ONHD (diameter >0≤221 μm, n=8) and large ONHD (diameter>221μm for left eyes.

Partial ETA squared (effect size) of 0.055 and 0.064 or right and left eyes respectively, means that 5.5 % and 6.4% of the variability in Global RNFL is accounted for by the group membership, which further means that increasing diameter of the ONHD has a small to moderate effect on the RNFL.

Table 11: Mean global RNFL thickness for different groups by ONHD diameter.

Mean global RNFL (µm)	Right eyes (±SD)	Left eyes (±SD)
No ONHD	102.2 (±11.0) µm *n=276*	102.0 (±11.1) µm *n=276*
Small ONHD	90.5 (±24.7) µm *n=9*	100.6 (±17.8) µm *n=8*
Large ONHD	89.3 (±26.1) µm *n=9*	84.2 (±22.7) µm *n=9*
p-value	p=0.180	p=0.119

P-value calculated using Welch's ANOVA.
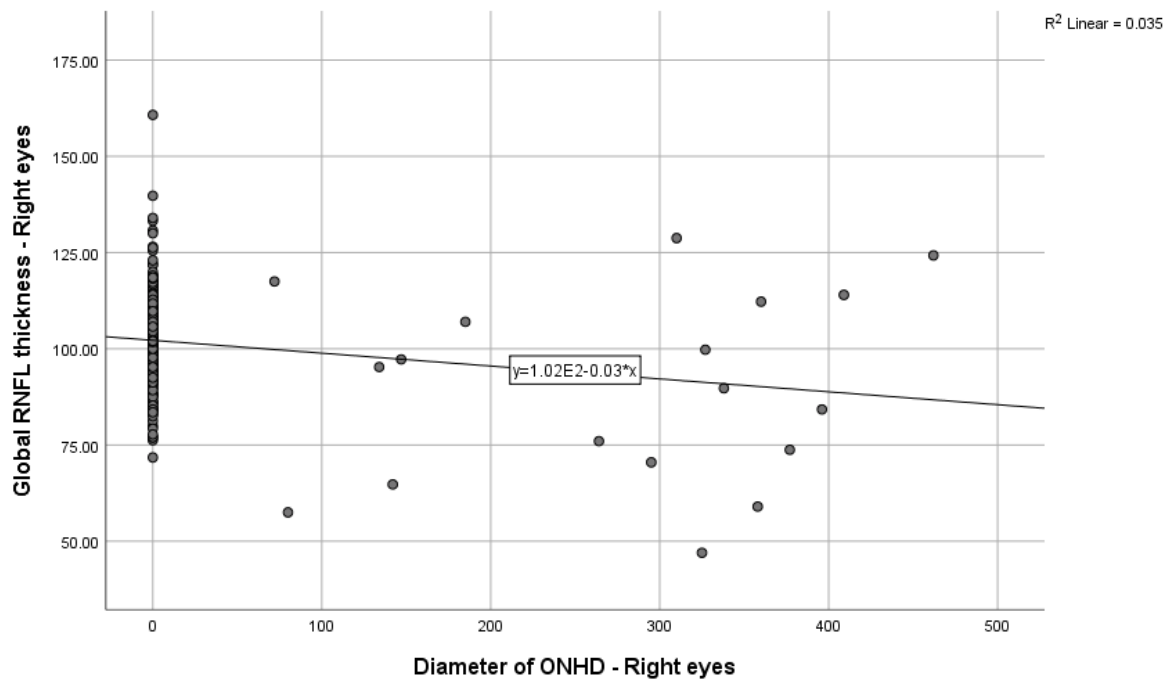
Figure 16: The figure shows the global RNFL thickness versus the ONHD diameter in µm, right eyes ($R^2=0.035$).
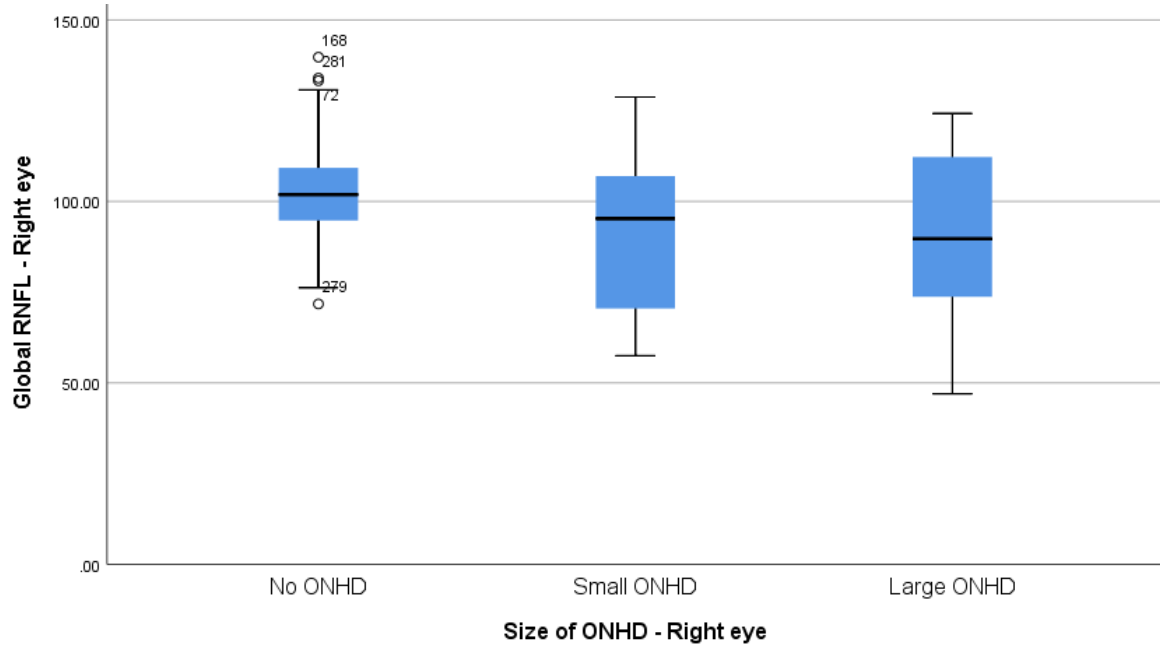
Figure 17: Size of ONHD's effect on Global RNFL, right eyes.

ONHD divided into groups by size; No ONHD (diameter=0, n=277), Small ONHD (diameter >0≤310 μm, n=9), Large ONHD (diameter>310μm, n=9).
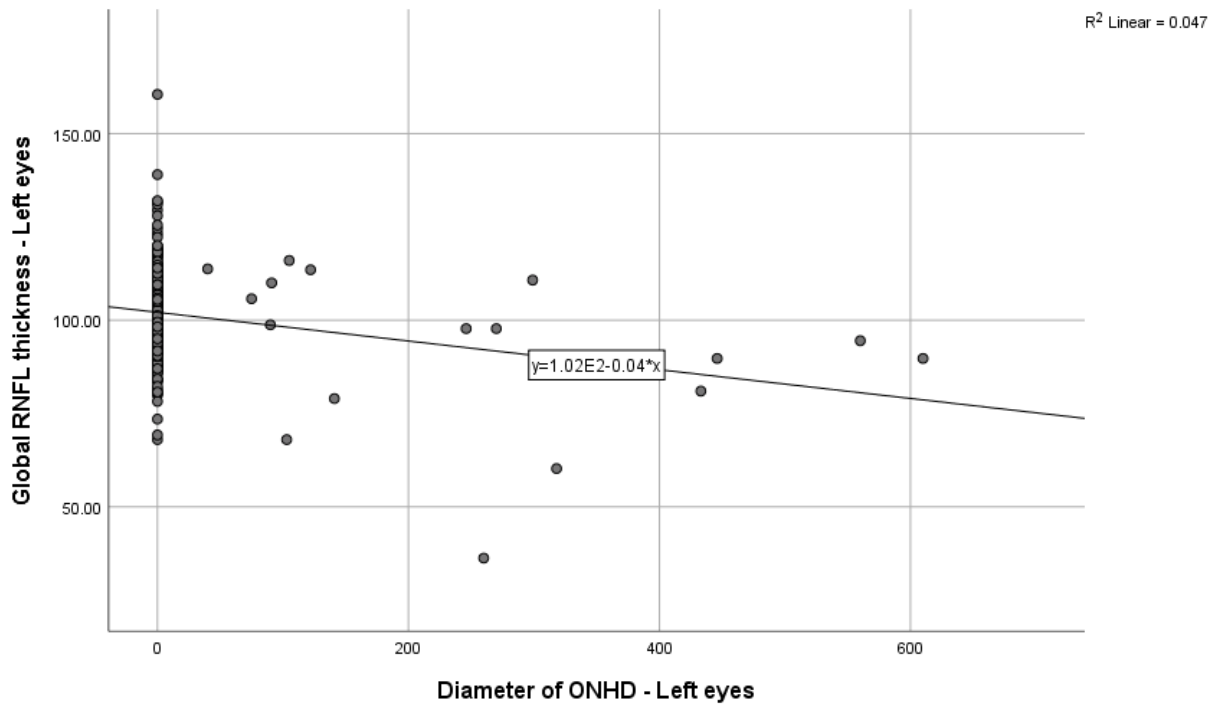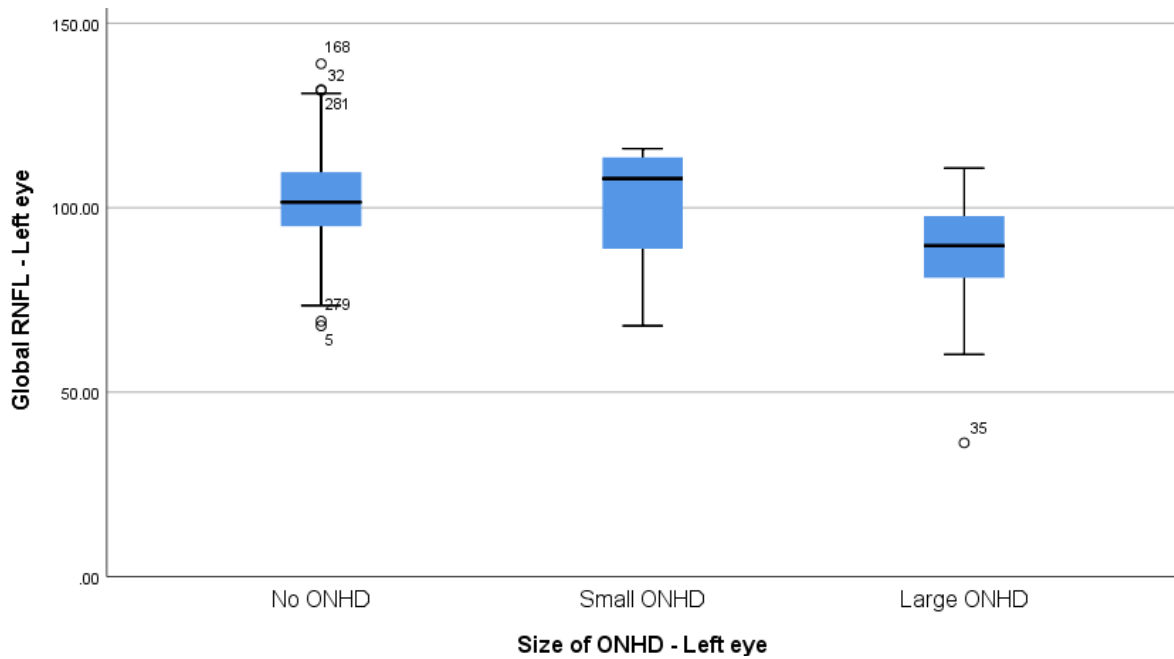
Figure 18: The figure shows the global RNFL thickness (μm) versus the ONHD diameter (μm), left eyes (R^2=0.047).

Figure 19: Size of ONHD's effect on Global RNFL, left eyes.

ONHD divided into groups by size; No ONHD (diameter=0, n=277), Small ONHD (diameter >0≤221 μm, n=8), Large ONHD (diameter>221μm, n=9).

3.6 Quantity of ONHD's effect on RNFL

When comparing mean global RNFL thickness between groups with different quantities of ONHD for right eyes, there was a statistically significant negative correlation between the global RNFL thickness and quantity of ONHD (p<0.005), the correlation applied "NO ONHD" and "Many ONHD", and "Few ONHD" and "Many ONHD", Table 12. This indicates a decreasing thickness of the RNFL with increasing quantity of ONHD. For left eyes there was only a slight trend towards thinner RNFL with increasing quantity of ONHD (p=0.151), Table 12, graph 20 and 21 below. The group with few ONHD had >0≤3 ONHD and the group with many ONHD had >3 ONHD.

A comment on the different results: The variability between the different groups for left eyes was heterogenic compared to the homogenic variability between the different groups for right eyes - which is the main reason for the different outcomes between right and left eyes when it comes to significant correlation.

The effect size was 0.209 for right eyes and 0.058 for left eyes, this means that 20.9% and 5.8% of the variability in global RNFL is accounted for by the group membership. For right eyes the increased quantity of ONHD had a large effect on RNFL, while for left eyes it only had a small to moderate effect on RNFL.

Table 12: Global RNFL thickness for different groups by quantity of ONHD.

"Few ONHD" means quantity>0≤3, "many ONHD means quantity>3.

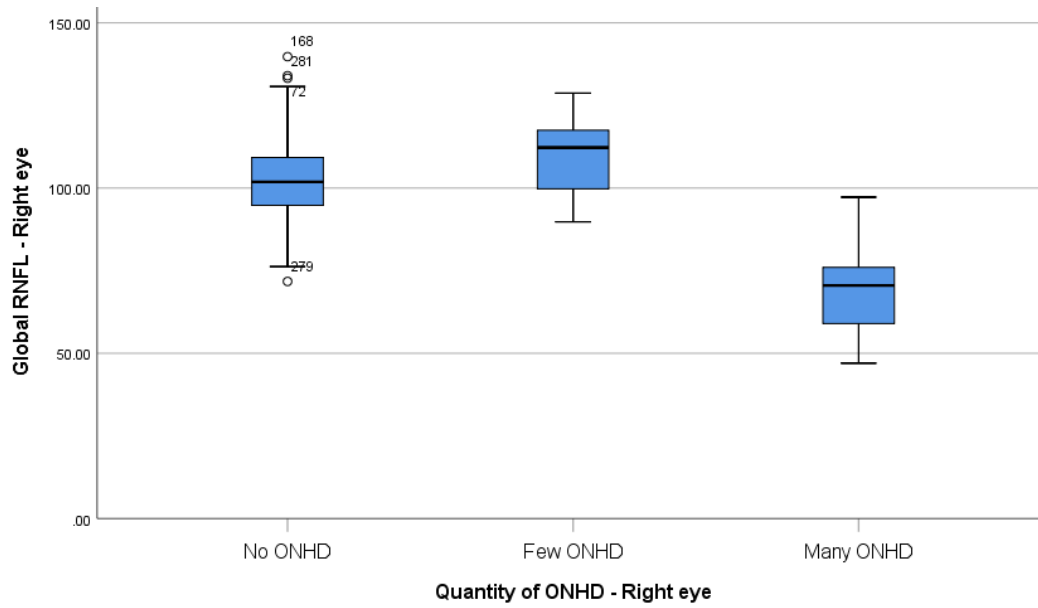| Mean global RNFL (μm)	Right eyes (±SD)	Left eyes (±SD)
No ONHD	102.2 (±11.1) *n=276*	102.0 (±11.1) *n=276*
Few ONHD >0≤3	109.8 (±13.1) *n=9*	101.6 (±17.4) *n=6*
Many ONHD >3	70 (±15.1) *n=9*	86.6 (±22.6) *n=11*
p-value	p<0.005	p=0.151

P-value calculated using Welch's ANOVA.

Figure 20: Global RNLF by quantity of ONHD, right eyes.

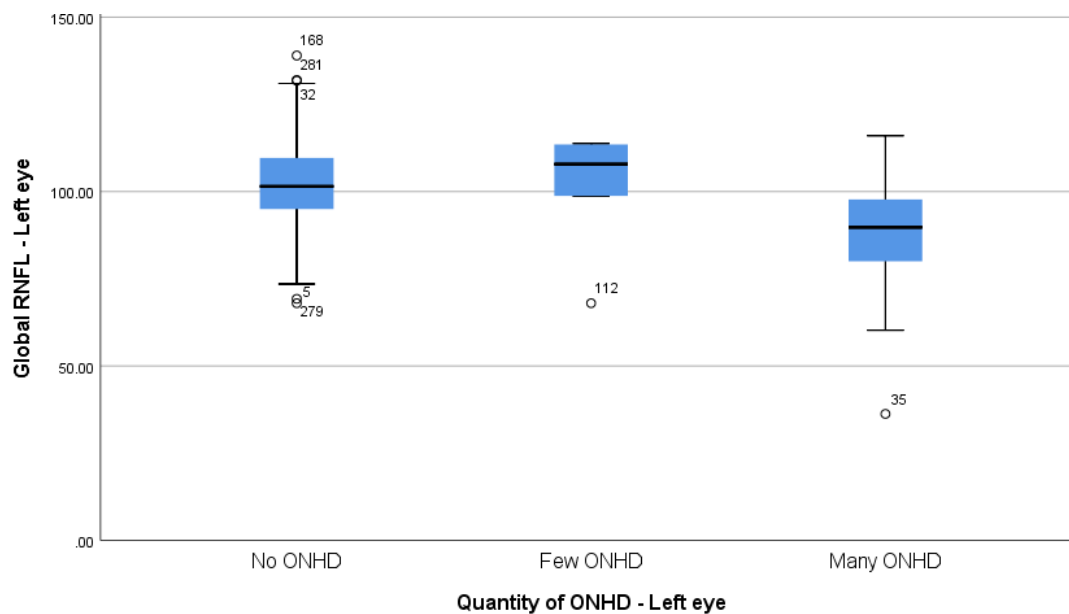*"No ONHD" (quantity=0, n=277), Few ONHD (quantity>0≤3, n=9), Many ONHD (quantity>3, n=9).*

Figure 21: Global RNLF by quantity of ONHD, left eyes.

"No ONHD" (quantity=0, n=277), "Few ONHD" (quantity>0≤3, n=6), "Many ONHD" (quantity>3, n=11).

3.7 Disc diameter in subjects with and without ONHD

The vertical disc diameter of eyes with ONHD for right eyes was 1646.6 (±232.0) µm which was slightly larger than normal group with 1595.3 (±194.4) µm (p=0.272). The opposite for left eyes; where disc diameter in eyes with ONHD was 1612.4 (±238.6) µm which was slightly smaller than disc diameter in the normal group with 1623.5 (±188.2) µm (p=0.812), Table 13, and Figure 22 and 23.

Table 13: Summary of disc diameter for normal group and group with ONHD.

Mean disc diameter (µm)	No ONHD (±SD)	ONHD (±SD)	p-value
Right eyes	1595.3 (±194.4) *n=285*	1646.6 (±232.0) *n=19*	p=0.272
Left eyes	1623.5 (±188.2) *n=285*	1612.4 (±238.6) *n=18*	p=0.812

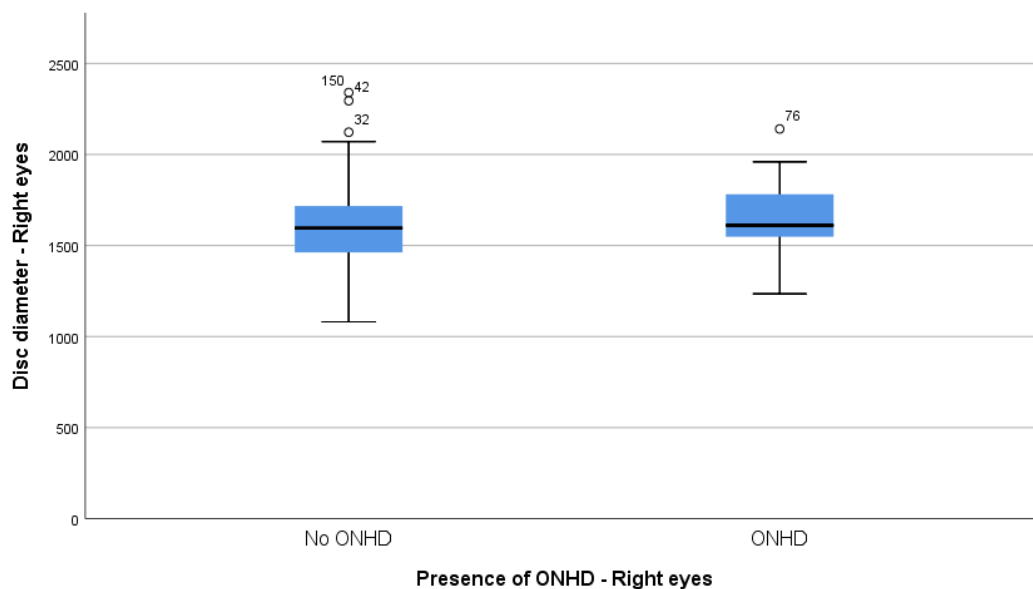*P-value calculated using independent T-Test.*

Figure 22: Disc diameter, right eyes

The mean disc diameter is marginally larger for the ONHD group compared to the normal group. Normal group =" No ONHD" and ONHD group = "ONHD".
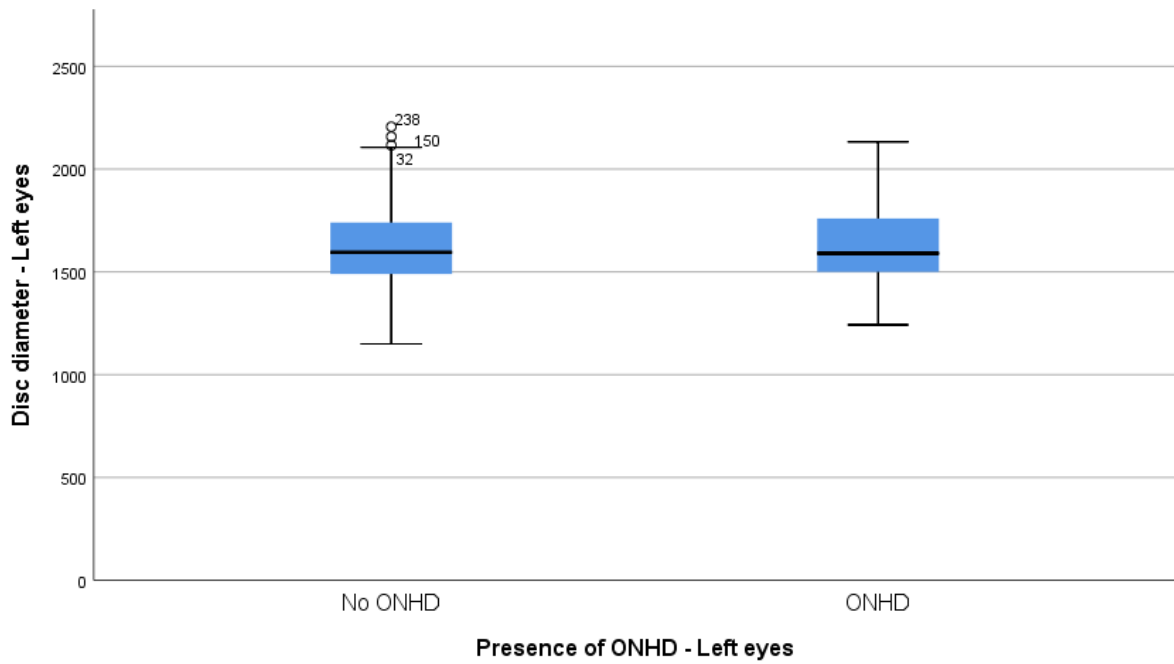
Figure 23: Disc diameter, left eyes.

The mean disc diameter is marginally smaller for the ONHD group compared to the normal group. The mean disc diameter is marginally larger for the ONHD group compared to the normal group. Normal group =" No ONHD" and ONHD group = "ONHD".

3.8 Uncertain diagnose

One of the 305 participants had some black holes/spaces in the inferior quadrant in the RNFL in the ONH which were not hyperautofluorescent with AF-imaging. The RNFL were thinner than for the normal group, but the participant had good visual acuity and were healthy (Figure 24). This patient was investigated further, but not registered as eye with ONHD.
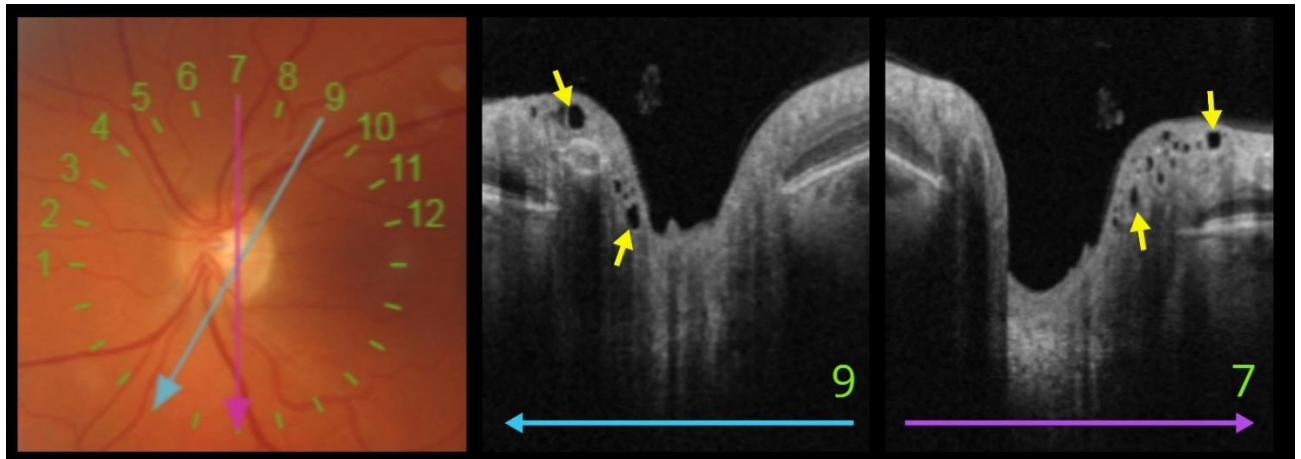

Figure 24: Differential diagnose to ONHD

Left image show ONH (left eye, id nr.80) with lines that illustrates the centration of the OCT-scan pattern. The blue and purple line indicates the position of the OCT-scan shown in the middle and to the right. On the OCT-scans we observe some small holes (yellow arrows) which were only present in the inferior quadrant in the left eye in this participant.

4 Discussion

The main objective of this study was to find the prevalence of ONHD in a Norwegian population using different methods; OCT, AF-imaging, and photography, and to compare the results found with the different modalities. To the best of my knowledge, there is no similar study performed earlier.

The prevalence of ONHD in this study was 7.5% measured with SD-OCT, 3.3% measured with fundus photography and 7.2% measured with AF (Optomap). As described earlier, the diagnostic criteria for ONHD with OCT was a mass with a signal-poor core (hyporeflective) surrounded by a hyperreflective margin, full or partial, as previously reported (Hamann et al., 2018; Sato et al., 2013; Wang et al., 2018). With fundus photography, the visible ONHD were defined as bright yellow, irregular deposits within the optic nerve head, or on the disc margin (Lorentzen, 1966). With AF-image the ONHD were defined as hyperfluorescent parts of the optic nerve head.

A small collection that shows the appearances of ONHD with the different methods are shown in Figure 8.

The prevalence of ONHD in previous studies varies according to which method used to examine the ONH. Histological studies with large study samples have found ONHD in 1.8% to 2.04% of the study population (Friedman et al., 1975; Skougaard et al., 2019), and studies where the ONH was only visually examined with photography or ophthalmoscopy, a prevalence of 0.2% to 0.3% was found (Lorentzen, 1966; You et al., 2009), which also is lower than the reported prevalence in the present study.

There are just a few studies concerning prevalence of ONHD with OCT. A large study on ONHD in children (mean age: 11.4 years) found a prevalence of 1% (Malmqvist et al., 2017c). They used a radial scan with 30 degrees spacing between each section compared to 15 degrees in the present study, therefore some ONHD may have been missed. Ghassibi et al. (2017) found ONHD in 14.6% of 130 normal subjects using EDI-OCT - which is considerably higher than any of the previous research – though, they included horizontal hyperreflective bands anterior to the lamina cribrosa in the definition of ONHD, illustrated in Figure 25. It is uncertain if these actually are a ONHD in formation, conglomerates of small ONHD or a part of the lamina cribrosa, and until further longitudinal studies are performed, it is advised to not diagnose as ONHD (Malmqvist, Bursztyn, et al., 2017).

In the present study the prevalence is higher than previously reported by histological studies, and there is some uncertainty about the smallest ONHD detected in 3 participants (Figure 25), if they are ONHD or the hyperreflective bands described earlier. Still, there was observed a small hyporeflective mass anterior to the hyperreflective part (Figure 25), similar to findings by (Sato et al., 2013), Figure 26. In addition, all the participants with the uncertain ONHD had large ONHD in the other eye, therefore the prevalence of subjects with ONHD would not have changed. There is reported ONHD as small as 5 µm, measured histologically (Tso, 1981), which supports the inclusion of the small ONHD (<123 µm) in this study. With OCT, ONHD were bilateral in 60.9% of the ONHD subjects. A study also using SD-OCT have reported 89% of ONHD were bilateral (Gili, Flores-rodríguez, Martin-ríos, et al., 2013) and others using EDI-OCT have found that 61% of ONHD in children and 95% of ONHD in adults were bilateral. The result from our study is in the lower part of what is previously reported, and it is possible that some small and deep ONHD were not detected because we used SD-OCT, mainly because of lower resolution in the deeper part of the ONH.
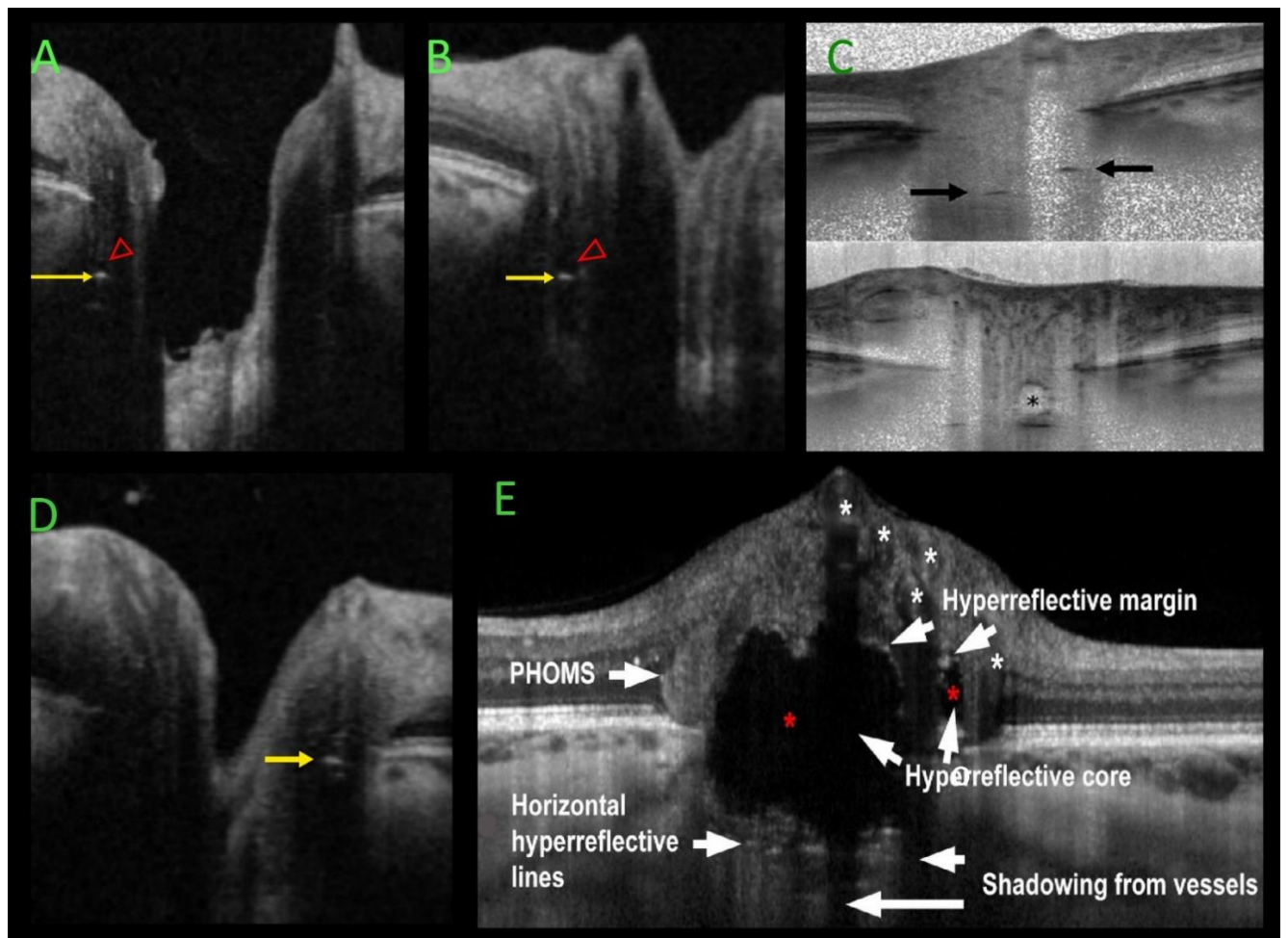
Figure 25: Shows illustrations of OCT-scans of ONH to compare the small ONHD only detected with OCT.

These ONHD are marked with red arrowheads (A=left eye, id.nr 140, B=left eye, id.nr. 225, D=right eye, id.nr. 289) and the hyperreflective bands marked with black arrows (C) and white arrow (E) found in earlier studies. C and E are illustrations from C= (Ghassibi et al., 2017) and E=(Malmqvist, Bursztyn, et al., 2017) where EDI-OCT was used, and the visualization in the deeper part of the ONH is clearly improved. A and B shows a small hyporeflective mass (red arrowheads) anterior to the hyperreflective part (yellow arrows). These hyperreflective lines in C and E are similar to those found in A, B and D, but A and B have the small hyporeflective mass anterior (red arrowheads). D however seems almost identical but might be RPE that continues after the shadow from the blood vessel. Still, there is a small hyporeflective part anterior to the hyperreflection that could be the ONHD, in addition the hyperreflections above and under does not seem like RPE. All the subjects (A, B, and D) have larger and more certain ONHD in the other eye.
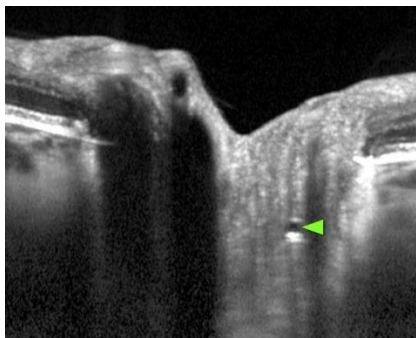

Figure 26: Small ONHD (green arrowhead). (Sato et al., 2013).

In this study there was a higher portion of female participants (61.3%) than male participants (38.7%). This might affect the result as ONHD is occurring more often in females than males (Gili, Flores-rodríguez, Martin-ríos, et al., 2013). Of the participants with ONHD, 69.6% of the participants were female and 30.4% were male, which is close to previous distribution reported by Sato et al. (2013) who found a distribution of 60% females and 40% males of participants with ONHD.

To estimate the difference between the methods, AF-image and photography was each compared to OCT. It was done this way since all the ONHD detected with AF-image and photography also were detected with OCT – therefore used as the valid method in this case.

In eyes with ONHD detected with OCT, 89.5% of right eyes and 77.8% of left eyes were also detected with AF. This is considered as an almost perfect agreement when comparing the two methods, and is consistent with the result from Sato et al. (2013) who found a sensitivity of 88.5%, when comparing OCT and AF. Still, the degree of hyperautofluorescence varied greatly, Figure 27. The varying intensity is either due to overlying tissue (deeper ONHD) or less calcified margins, where the latter is more common in children (Chang & Pineles, 2016). In a study by Gili, Flores-Rodríguez, Yangüela, et al. (2013), they found an excellent inter-observer agreement between observers with different experience. The study had the same weakness as this; the whole ONH were evaluated, not the corresponding quadrants. For example, in Figure 27, the ONH have obvious hyperautofluorescence in the superior quadrant but it is not as obvious in the inferior quadrant. Therefore, we believe that the method depends on an observant observer.

Furthermore, all the visible ONHD were hyperautofluorescent and the buried ONHD were hyperautofluorescent in 84.6% and 60% of right and left eyes respectively, and 73.9% when counting total number of eyes with buried ONHD. This correlates with previous findings where eyes with visible ONHD showed hyperautofluorescence in 93-100% (Gili, Flores-Rodríguez, Yangüela, et al., 2013; Pineles & Arnold, 2012) and eyes with buried ONHD showed hyperfluorescence in 50-92% (Gili, Flores-Rodríguez, Yangüela, et al., 2013; Kurz-Levin & Landau, 1999).

Eyes with ONHD detected with OCT that were not detected with AF-image, all had in common: few ONHD, smaller ONHD (<123µm), ONHD with weaker hyperreflective margin anteriorly, ONHD location posterior to Bruch's membrane (Figure 9), and thicker RNFL than ONHD that were detected with AF-image. Although the ONHD with no hyperautofluorescence were located posterior to Bruch's membrane and were small in size, the hyperfluorescence does not seem to be a reliable indicator of the vertical location or the size, since several hyperautofluorescent ONHD are located deeper within the scleral canal (Figure 27) or have a small diameter (<105 µm). In previous studies, large and diffuse hyperfluorescence have shown to correspond with large and deep ONHD (Malmqvist, Bursztyn, et al., 2017). This suggests that the brightness and area of hyperfluorescence will give an indication of location and size, but still there may be ONHD present that only will be visible with OCT as illustrated in Figure 9.
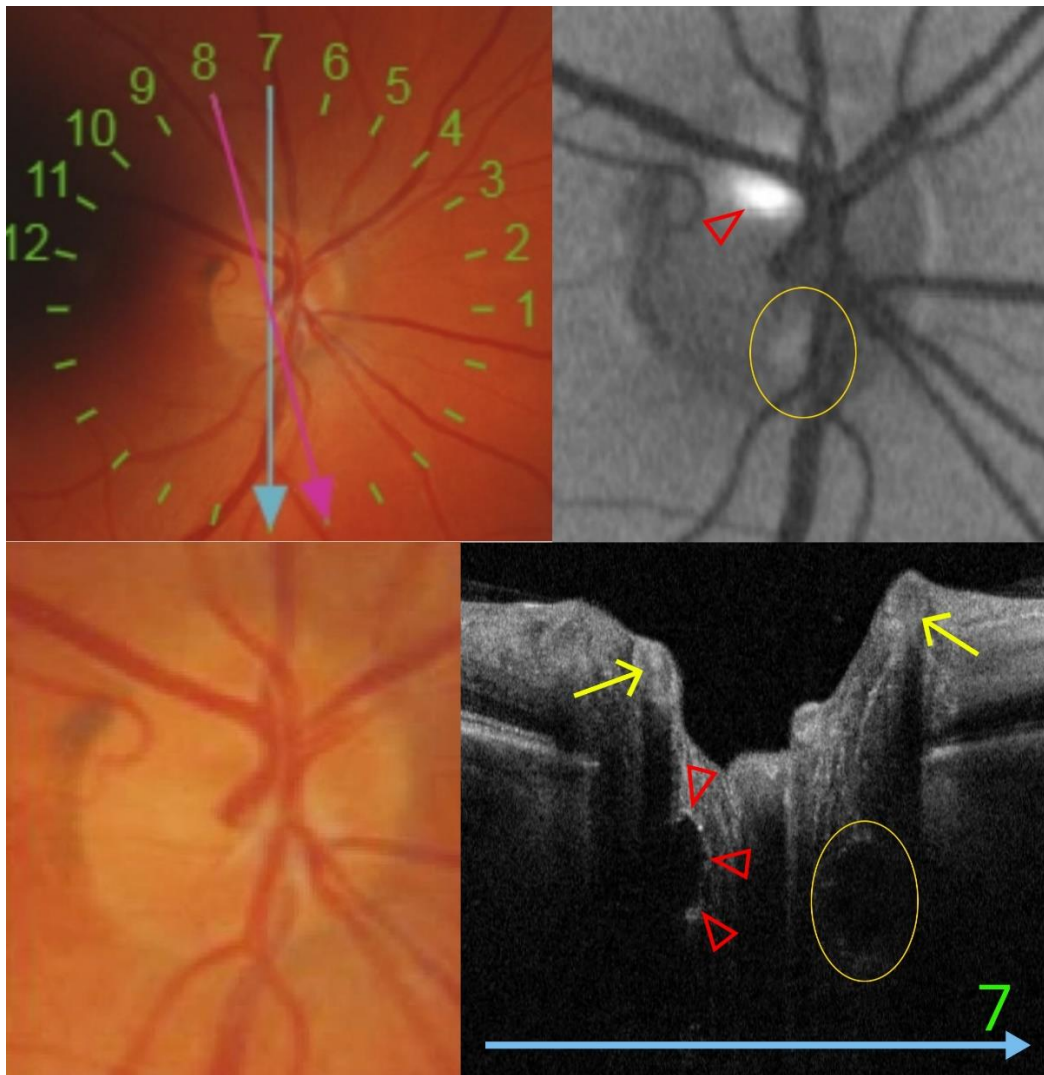
Figure 27: Varying hyperautofluorescence

The top right image shows an AF-image of an ONH (right eye, id nr 46) where there is a bright hyperautofluorescent area at 11 o'clock (red arrowhead). If you look carefully, there is an additional hyperautofluorescent area below this, at 6 o'clock (yellow circle). The top left image illustrates the centration of the OCT-scan pattern, and the blue line indicates position of the OCT-scan illustrated at the bottom right. The red arrows indicate the location of the superior ONHD (located 11 o'clock), and the yellow circle the inferior ONHD (6 o'clock position). The difference in hyperautofluorescence found here is most likely due to varying thickness in overlying tissue and difference in vertical position (in depth). Yellow arrows marks vessels that

cause posterior shadowing. Bottom left image is the photo of the ONH, where it is difficult to detect any ONHD.

In eyes with ONHD detected with OCT, 31.6% of right eyes and 44.4% of left eyes had visible ONHD when assessing the photography of the ONH. These findings are reasonably close to what other studies have reported, where 21% to 30.8% of eyes with ONHD had visible ONHD (Sato et al., 2013; Teixeira et al., 2019). The first study, where they found 21% visible ONHD, was conducted on subjects under 18 years old where the mean age was higher for the subjects with visible ONHD (14±4) than the subjects with buried ONHD (11±4) (Teixeira et al., 2019). The study population in the present study is adults over 18 years old and had a higher mean age than these two studies, and since the ONHD evolve and typically becomes visible at an age of 12 (Hoover et al., 1988) we would expect a higher prevalence of visible ONHD than the studies performed in children. However, in our study, the difference in age was not statistically significant between buried ONHD and visible ONHD. An assessment of 1713 enucleated eyes found that 23% of ONHD were superficial, meaning here; they were located above the Bruch's membrane (Skougaard et al., 2019), so this is not completely comparable to our study. The term 'superficial' is often mixed up in literature as 'visible', which may be misleading because the ONHD located above Bruch's membrane is not necessarily visible on photo or ophthalmoscopy, as illustrated in Figure 28.

The eyes with ONHD not detected with fundus had varying vertical location but had in common tissue covering the ONHD. In some eyes, the anterior border of the ONHD was located anterior to the Bruch's membrane (Figure 28) and in other eyes the ONHD was located deeper within the ONH (Figure 27).
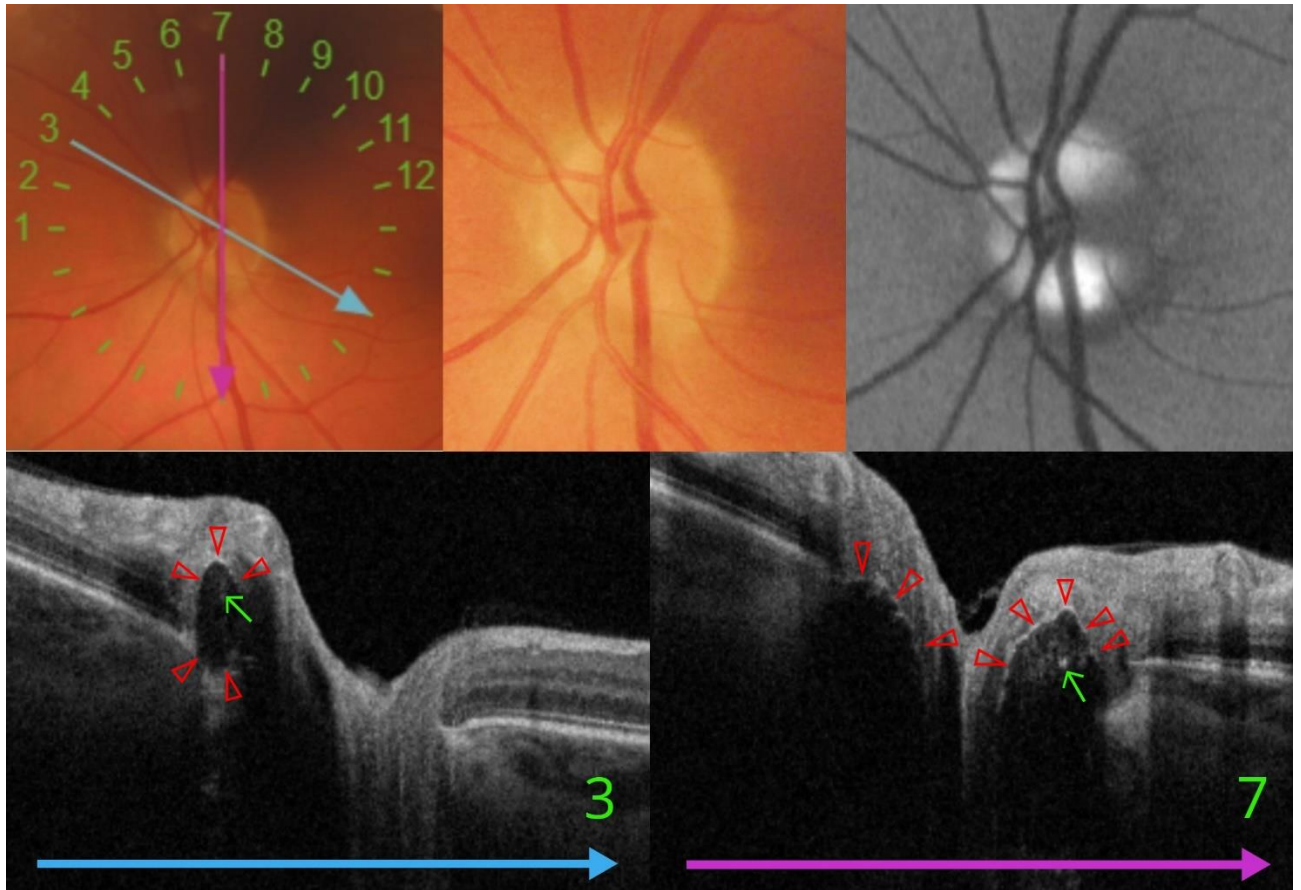
Figure 28: Images of ONH (left eye, id nr: 153)

The AF-image (top, right) show hyperautofluorescence from 5 to one o'clock with brightest hyperfluorescence at 10 o'clock and between 5 and 6 o'clock. The top left image illustrates centration of the OCT-scan pattern, where both lines (blue and purple) indicates position of the OCT-scans illustrated below. On the bottom left image there is an ONHD (red arrowheads) mainly located anterior to the Bruchs membrane where both the anterior and the posterior margin is detected. In addition, there is a small hyperreflective foci internally (green arrow). The bottom right image shows two large ONHD where only the anterior margin is detected by the OCT (red arrowheads), the lack of visualization of the posterior part makes it difficult to determine largest diameter. Small, hyperreflective foci internally (green arrow). The photo of the ONH (top, middle) show no clear ONHD, but a slightly brighter area at 8 o'clock, which was not registered as ONHD.

Ideally, the presence of ONHD should have been confirmed by an instrument regarded as "Gold standard"; Enhanced Depth Imaging-OCT, Swept Source OCT or B-scan Ultrasound. B-scan Ultrasound may miss ONHD with less calcification, and therefore the Enhanced Depth Imaging-OCT and Swept Source OCT is the preferred technique - also due to improved

detection of the deepest border of the ONHD compared to normal vitreal SD-OCT imaging (Merchant et al., 2013).

The difference in detection of ONHD between the different methods would have been more accurate if the interrater reliability had been compared by quadrant and not the whole ONH. In addition, intra-rater reliability could have been performed to give an estimation about the sensitivity of the operator. This would have given information about how well and consequent the operator graded the images and scans. Alternatively, one additional operator could have been recruited, and the grading could have been compared. As for the assessment of the images; all the images for each participant were assessed in this specific order; fundus photography, OCT, AF-image. This order was chosen because the ONHD detection with fundus photography were expected to be lowest, and an assessment of the AF-image or OCT-scan prior to the photos would lead to bias. However, a better way would have been to assess each method separately; the fundus images for all participants, then the OCT scans for all participants, and last, the AF-images for all participants. In that way, assessment-bias would be eliminated.

The second objective of this study was to investigate the characteristics of the optic nerve head drusen found in the same population.

The mean greatest diameter of ONHD of 267.42 um and 244.78 um for right and left eyes respectively, is smaller compared to 686,8±395,2μm that Sato et al. (2013) found when using EDI-OCT. The difference may be due to different sample inclusion since half of their ONHD sample was included based on hyperautofluorescent ONH using fundus autofluorescence, which means that the ONHD diameter were larger than if the inclusion was based on detection with OCT, since the hyperautofluorescent ONHD are larger, as found in our study. In addition, lack of visualization in the deepest margin of the ONHD in some of the ONHD eyes may also have contributed to smaller estimation of the diameter (Figure 28), which is known from other studies using SD-OCT (Merchant et al., 2013). The determination of ONHD diameter in this study was made by simply measuring the greatest observed diameter on the 12 different sections on the radial scan with OCT. Since the ONHD are irregular masses, the diameter as a measure of size may not be a representative indicator of the ONHD volume, especially if the horizontal diameter is greater than the vertical diameter. There were no available programs for determining volume in the software used in this study. Posterior shadowing from vessels may also be a reason for inaccurate measurements as we lack information from the tissue beneath the vessels, Figure 27). The ONHD that was not detected with AF-imaging had a significantly smaller diameter than the ONHD detected with AF-imaging. As we also found in this study,

clinically visible ONHD are reported to be significantly larger than buried ONHD (Malmqvist, Lindberg, et al., 2017).

For all detection methods used, ONHD was least present in the temporal quadrant of the ONH. Measured with OCT in a study concerning children (<18 years), ONHD were more commonly found in the nasal (61%), inferonasal (55%) and superonasal (40%) sectors using OCT (Teixeira et al., 2019).

The RNFL thickness has been reported to be reduced in all sectors except the temporal, where the largest reduction was found in the nasal and superior section (Gili, Flores-rodríguez, Martin-ríos, et al., 2013). This correlates to our finding concerning the location of the ONHD, since they seem to be less likely to form in the temporal part, they do not affect this part of the ONH. In our study, we only compared the global RNFL.

Global RNFL thickness in subjects with ONHD is previously reported to be thinner than in normal subjects (Gili, Flores-rodríguez, Martin-ríos, et al., 2013), which was also tested among our subjects. We found a trend towards reduction of global RNFL thickness in the subjects with ONHD compared to the normal group, but it was not significant. If we compared all the subjects with either positive or negative hyperautofluorescence in the ONH – the RNFL was significantly thinner in the group with hyperfluorescent ONH. The same was for eyes with visible ONHD compared to ONH were no ONHD could be seen – the RNFL was thinner in the group with visible ONHD. Therefore, the method of detection could indicate different levels of damage to the RNFL, which also would be helpful in lack of an OCT. This should be investigated further in a study with larger sample sizes.

Eyes with visible ONHD had a significantly thinner RNFL than eyes with buried ONHD for right eyes. For the left eyes it was lower but not significant. Eyes with ONHD not detected with AF had a thicker RNFL than eyes with hyperfluorescent ONHD. This confirms what earlier mentioned, that these drusen were either small or just a few, and thus probably affect the RNFL less than the visible ONHD and the buried ONHD detected with AF-image.

The different ONHD diameter had no significant effect on the RNFL thickness in this study.

In a study performed by Sato et al. (2013) there was a significant negative correlation between greatest ONHD diameter and RNFL, however, the mean greatest ONHD diameter was over two times larger than this study, which may have been a leading factor. Other studies have found decreased global RNFL and worsening of mean deviation (visual field defects) with

increasing volume of ONHD (Malmqvist, Lindberg, et al., 2017; Tsikata et al., 2017), which was not investigated in this study. As pointed out, since the ONHD are irregular masses, the greatest diameter measured in the present study, may not give a correct indication of the ONHD volume in all cases. It might be that increasing size in the horizontal direction affects the RNFL more than masses in the vertical direction will affect the RNFL.

In lack of possibility of measuring the ONHD volume, further studies could measure both horizontal- and vertical diameter to see which have greatest effect on the RNFL.

Regarding the quantity of ONHD and the effect on the global RNFL, the results were different for right and left eyes. For right eyes, there was a statistically significant negative correlation between the global RNFL thickness and quantity of ONHD, which indicates a thinning of the RNFL with increased quantity of ONHD, similar to previous findings (Roh et al., 1998). Still, even if not significant, there was a trend towards thinner RNFL with increasing quantity of ONHD also for the left eyes.

The quantity of ONHD was divided in 50% percentile by median where "Many ONHD" were all eyes with over three ONHD; this have perhaps made the two ONHD groups too similar. It may have improved the output information if the groups were divided in several groups. Another error source is the use of radial scan to detect ONHD, where for example if ONHD is detected in several neighbouring sections, it is difficult to distinguish if there are one large ONHD or several ONHD.

The vertical disc diameter was not significantly different between eyes with ONHD compared to eyes without ONHD. The results were contradictory for right and left eyes, where vertical disc diameter for right eyes with ONHD were slightly larger compared to the normal group and the opposite for left eyes with a slightly smaller disc diameter for ONHD group. The previous research using OCT are inconclusive; scleral canal size is both found to be significantly larger (Flores-Rodríguez et al., 2013) and significantly smaller (Malmqvist et al., 2017c) in ONHD subjects. The disc diameter is, with OCT, defined as the opening in the Bruch's membrane and the measurement depends on the visibility of the edge, which might be blurred from overlying structures and lead to imprecise estimates. The disc diameter could have made a more accurate measure of scleral canal size if mean of horizontal –and vertical diameter had been calculated, instead of just the vertical diameter as measured in our study.

The peripapillary hyperreflective mass (PHOMS) described as buried ONHD (Chang & Pineles, 2016; Gospe et al., 2016; Min Lee, Woo, & Hwang, 2013; Rebolleda et al., 2015), and the hyperreflective bands (Ghassibi et al., 2017), are not counted as ONHD in this study as there is no evidence that these are ONHD (Hamann et al., 2018; Malmqvist, Sibony, et al., 2018; Wang et al., 2018). However, some of the ONHD that were not hyperautofluorescent with AF-imaging in the present study (described above) are small and the diagnosis is uncertain due to reduced image resolution, which would have been increased with for example EDI-OCT or SS-OCT.

If PHOMS also had been counted as ONHD in our study; 41 subjects (13.4%) would have had ONHD in one or both eyes. PHOMS is often found together with ONHD and 14 of subjects with ONHD in the present study had coexisting PHOMS, see illustration Figure 29.

There was another uncertain diagnose where "empty" black holes were present in the inferior quadrant of the ONH (Figure 24). From the totally black internal colour, with no hyperreflective margin as, it does not seem like an ONHD, but might resemble cysts within the RNFL. In addition, the holes were not hyperfluorescent with AF-imaging, as we would expect if they were ONHD located at this level in the ONH. Otherwise, this participant was healthy, had good visual acuity, but lower mean RNFL than normal group in both eyes. As this may look as ONHD at the first glance, AF-image with no hyperfluorescence makes us think otherwise. This patient was investigated further, but not registered as eye with ONHD. This shows the importance of multimodal imaging.

Eyes with ONHD that were not detected with AF-imaging, both had significantly smaller ONHD diameter and a significantly thicker RNFL than ONHD eyes that showed hyperautofluorescence. In view of this, it may be interpreted that the eyes with no hyperautofluorescence on AF-image, will have less damage on the RNFL – at least from ONHD – and in case of much thinner RNFL in these clients, other reasons, like for example glaucoma, should be considered.
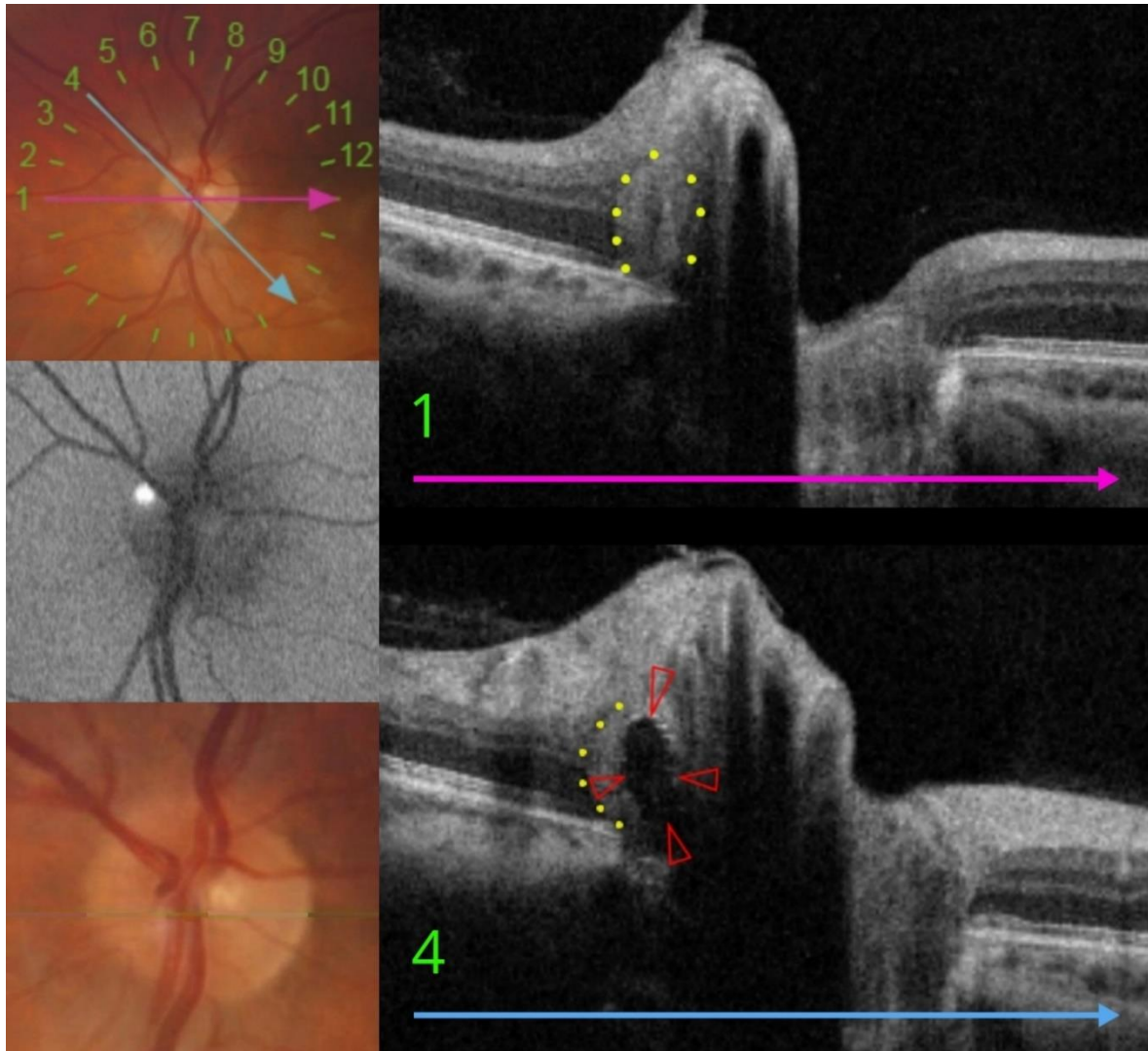
Figure 29: PHOMS vs ONHD

The top left image shows an ONH (left eye, id nr.27) with lines that illustrates centration of the OCT-scan pattern. The purple and blue line indicate position of OCT-scan illustrated respectively top right and bottom right. The middle left image shows an AF-image of the same ONH, where there is bright hyperautofluorescence at 10 o'clock, but no hyperautofluorescence at 9 o'clock which corresponds to the OCT-scan on the top right. Peripapillary hyperreflective ovoid mass-like structures (PHOMS) is outlined with yellow dots on both OCT-scans (right side), and one ONHD highlighted with red arrowheads (bottom right). Of ONHD and PHOMS it is only the ONHD that shows hyperautofluorescence. Bottom left fundus photo shows no obvious ONHD, but if we compare the location of the hyperautofluorescence on AF-image, the

corresponding area on the fundus photo might appear slightly brighter. However, it was not registered as visible ONHD.

Since ONHD is known to cause both afferent and retrobulbar axonal degeneration similar to glaucoma (Chan et al., 2017), follow-up should include monitoring of visual fields and OCT over time to measure the structure and function relationship, where the nasal part of the retina is important to emphasize (Skaat et al., 2017). As reported in another study, the long-term progression in the visible ONHD's volume and quantity, and further effect on the RNFL, is small (Malmqvist, Lund-Andersen, et al., 2017). We do not know if this also is the case for ONHD located deeper within the ONH, since the OCT-technology is relatively new, but this is also something to further investigate. Norwegian optometrists have access to varying instruments, but in cases of doubt where it is difficult to differentiate between ONHD and for example ODE, it is sensible to refer to an ophthalmologist.

In addition to RNFL thickness, some studies have measured the thickness of either ganglion cell-inner plexiform layer (GCIPL) (Casado et al., 2014) or macular ganglion cell layer (GCL) (Malmqvist, Lindberg, et al., 2017), and both suggests that these measurements are more useful for detecting early damages in eyes with ONHD than the RNFL exam. Neither of these layers were measured in our study but this is something to investigate further.

Limitations in this study is the use of radial scan to detect ONHD, and it is possible that some drusen were too small to be detected because of distance between scans, still there is only 15 degrees between each scan, and other studies also investigating prevalence have used radial scans with 30 degrees between each scan (Malmqvist et al., 2017c).

Another limitation in this study is the relatively small sample size of 305 participants for reporting a prevalence. The study aimed for approximately 385 participants calculated using formula for calculating sample size (Daniel, 1999). This formula is used when the expected prevalence is low and unknown, however, from previous research we expect a prevalence <10% and therefore the formula becomes different; since the expected prevalence (P) is below 10%, it is recommended to use precision (d) as half of prevalence (P) (Naing, Winn, & Nordin, 2006). From previous studies, we may expect a prevalence around 2%.

This gives:

$$n = \frac{Z^2 \cdot P(1-P)}{d^2} = \frac{1{,}96^2 \cdot 0{,}02(1-0{,}02)}{0{,}01^2} = 752{,}95 \approx 753$$

which results in a larger sample size than originally calculated.

Keeping in mind that this study does not only look at prevalence, but in addition compare different imaging methods for detecting ONHD and investigates effect on RNFL with the different methods, the number of participants is adequate. Future prevalence studies should however aim for a larger study sample.

5 Conclusion

The prevalence of ONHD found in this study is higher than previously reported in the literature, although a larger sample size is warranted to transfer these numbers to the whole Norwegian population. The disc diameter does not show any correlation with the prevalence of ONHD. Increased quantity of ONHD have a larger effect on the RNFL than increased ONHD diameter. Autofluorescent imaging (AF) and SD-OCT have a high correlation where AF-imaging detects all the visible ONHD and the majority of the buried ONHD. Still, there may be some buried ONHD that are only detected with OCT, but these are expected to be of less clinical importance since they are both smaller and have less impact on the RNFL. Thus, AF and SD-OCT are imaging techniques that both have a high clinical value when diagnosing optic nerve head drusen.

References

Auw-Haedrich, C., Staubach, F., & Witschel, H. (2002). Optic Disk Drusen. *Survey of Ophthalmology, 47*(6), 515-532. doi:10.1016/S0039-6257(02)00357-0

Bellezza, A. J., Rintalan, C. J., Thompson, H. W., Downs, J. C., Hart, R. T., & Burgoyne, C. F. (2003). Deformation of the Lamina Cribrosa and Anterior Scleral Canal Wall in Early Experimental Glaucoma. *Investigative Ophthalmology & Visual Science, 44*(2), 623-637. doi:10.1167/iovs.01-1282

Browning, S. (2013). Widefield imaging of the peripheral retina. *The Optician, 246*(6430), 24-26,28-29.

Casado, A., Rebolleda, G., Guerrero, L., Leal, M., Contreras, I., Oblanca, N., & Muñoz-Negrete, F. J. (2014). Measurement of retinal nerve fiber layer and macular ganglion cell–inner plexiform layer with spectral-domain optical coherence tomography in patients with optic nerve head drusen. *Graefe's Archive for Clinical and Experimental Ophthalmology, 252*(10), 1653-1660. doi:10.1007/s00417-014-2773-5

Chaglasian, M., Fingeret, M., Davey, P. G., Huang, W.-C., Leung, D., Ng, E., & Reisman, C. A. (2018). The development of a reference database with the Topcon 3D OCT-1 Maestro. *Clinical ophthalmology (Auckland, N.Z.), 12*, 849-857. doi:10.2147/OPTH.S155229

Chan, G., Morgan, W. H., Yu, D. Y., & Balaratnasingam, C. (2017). Retrobulbar axonal degeneration due to optic disc drusen. *Clinical & Experimental Ophthalmology, 46*(5), 564-567. doi:10.1111/ceo.13137

Chang, M. Y., & Pineles, S. L. (2016). Optic disk drusen in children. *Survey of Ophthalmology, 61*.

Daniel, W. W. (1999). *Biostatistics: A Foundation for Analysis in the Health Sciences*: Wiley.

Duncan, J. E., Freedman, S. F., & El-Dairi, M. A. (2016). The incidence of neovascular membranes and visual field defects from optic nerve head drusen in children. *Journal of AAPOS, 20*(1), 44-48. doi:10.1016/j.jaapos.2015.10.013

El-Koofy, N., El-Mahdy, R., Fahmy, M. E., El-Hennawy, A., Farag, M., & El-Karaksy, H. M. (2011). Alagille syndrome: clinical and ocular pathognomonic features. *Eur. J. Ophthalmol., 21*(2), 199-206. doi:10.5301/EJO.2010.5675

Flores‐Rodríguez, P., Gili, P., Martín‐Ríos, M. D., & Grifol‐Clar, E. (2013). Comparison of optic area measurement using fundus photography and Optical Coherence Tomography between optic nerve head drusen and control subjects. *Ophthalmic and Physiological Optics, 33*(2), 164-171. doi:10.1111/opo.12017

Floyd, M. S., Katz, B. J., & Digre, K. B. (2005). Measurement of the scleral canal using optical coherence tomography in patients with optic nerve drusen. *American Journal of Ophthalmology, 139*(4), 664-669. doi:https://doi.org/10.1016/j.ajo.2004.11.041

Friedman, A. H., Gartner, S., & Modi, S. S. (1975). Drusen of the optic disc. A retrospective study in cadaver eyes. *British Journal of Ophthalmology, 59*(8), 413. Retrieved from http://bjo.bmj.com/content/59/8/413.abstract

Frisén, L. (2008). Evolution of drusen of the optic nerve head over 23　years. *Acta Ophthalmologica, 86*(1), 111-112. doi:10.1111/j.1600-0420.2007.00986.x

Ghassibi, M. P., Chien, J. L., Abumasmah, R. K., Liebmann, J. M., Ritch, R., & Park, S. C. (2017). Optic Nerve Head Drusen Prevalence and Associated Factors in Clinically Normal

Subjects Measured Using Optical Coherence Tomography. *Ophthalmology, 124*(3), 320-325. doi:10.1016/j.ophtha.2016.10.035

Gili, P., Flores-rodríguez, P., Martin-ríos, M. D., & Carrasco Font, C. (2013). Anatomical and functional impairment of the nerve fiber layer in patients with optic nerve head drusen. *Graefe's Archive for Clinical and Experimental Ophthalmology, 251*(10), 2421-2428. doi:http://dx.doi.org/10.1007/s00417-013-2438-9

Gili, P., Flores-Rodríguez, P., Yangüela, J., & Herreros Fernández, M. L. (2013). Using autofluorescence to detect optic nerve head drusen in children. *Journal of American Association for Pediatric Ophthalmology and Strabismus, 17*(6), 568-571. doi:https://doi.org/10.1016/j.jaapos.2013.07.012

Gili, P., Flores-Rodríguez, P., Yangüela, J., Orduña-Azcona, J., & Martín-Ríos, M. (2012). Sensitivity and specificity of monochromatic photography of the ocular fundus in differentiating optic nerve head drusen and optic disc oedema. *Incorporating German Journal of Ophthalmology, 251*(3), 923-928. doi:10.1007/s00417-012-2223-1

Gospe, S. M., Bhatti, M. T., & El-Dairi, M. A. (2016). Anatomic and visual function outcomes in paediatric idiopathic intracranial hypertension. In (pp. 505): BMJ Publishing Group Ltd.

Hamann, S., Malmqvist, L., & Costello, F. (2018). Optic disc drusen: understanding an old problem from a new perspective. *Acta Ophthalmologica, 96*(7), 673-684. doi:10.1111/aos.13748

Hoover, D., Robb, R., & Petersen, R. (1988). Optic Disc Drusen in Children. *Journal of Pediatric Ophthalmology and Strabismus, 25*(4), 191-195.

Katz, B. J., & Pomeranz, H. D. (2006). Visual Field Defects and Retinal Nerve Fiber Layer Defects in Eyes With Buried Optic Nerve Drusen. *American Journal of Ophthalmology, 141*(2), 248-253.e241. doi:10.1016/j.ajo.2005.09.029

Kim, K., Ahn, S., & Kim, D. (2013). Comparison of two different spectral domain optical coherence tomography devices in the detection of localized retinal nerve fiber layer defects. *The Official English-Language Journal of the Japanese Ophthalmological Society, 57*(4), 347-358. doi:10.1007/s10384-013-0239-7

Kurz-Levin, M. M., & Landau, K. (1999). A Comparison of Imaging Techniques for Diagnosing Drusen of the Optic Nerve Head. *Archives of Ophthalmology, 117*(8), 1045-1049. doi:10.1001/archopht.117.8.1045

Lam, B. L., Morais, C. G., & Pasol, J. (2008). Drusen of the optic disc. *Current Neurology and Neuroscience Reports, 8*(5), 404. doi:10.1007/s11910-008-0062-6

Landis, J. R., & Koch, G. G. (1977). The Measurement of Observer Agreement for Categorical Data. *Biometrics, 33*(1), 159-174. doi:10.2307/2529310

Lee, A. G., & Zimmerman, M. B. (2005). The Rate of Visual Field Loss in Optic Nerve Head Drusen. *American Journal of Ophthalmology, 139*(6), 1062-1066. doi:https://doi.org/10.1016/j.ajo.2005.01.020

Lee, K. M., Woo, S. J., & Hwang, J.-M. (2011). Differentiation of Optic Nerve Head Drusen and Optic Disc Edema with Spectral-Domain Optical Coherence Tomography. *Ophthalmology, 118*(5), 971-977. doi:https://doi.org/10.1016/j.ophtha.2010.09.006

Liu, B., Murphy, R. K. J., Mercer, D., Tychsen, L., & Smyth, M. D. (2014). Pseudopapilledema and association with idiopathic intracranial hypertension. *Child's Nervous System, 30*(7), 1197-1200. doi:10.1007/s00381-014-2390-y

Lorentzen, S. E. (1966). Drusen of the optic disk. A clinical and genetic study. *Acta Ophthalmol Suppl*.

Malmqvist, L., Bursztyn, L., Costello, F., Digre, K., Alexander Fraser, J., Fraser, C., . . . Hamann, S. (2018). Peripapillary Hyperreflective Ovoid Mass-Like Structures: Is It Optic Disc Drusen or Not? *Journal of Neuro-Ophthalmology, 38*, 1. doi:10.1097/WNO.0000000000000674

Malmqvist, L., Bursztyn, L., Costello, F., Digre, K., Fraser, J. A., Fraser, C., . . . Hamann, S. (2017). The Optic Disc Drusen Studies Consortium Recommendations for Diagnosis of Optic Disc Drusen Using Optical Coherence Tomography. *J Neuroophthalmol, 38*(3), 299-307. doi:10.1097/wno.0000000000000585

Malmqvist, L., Li, X. Q., Eckmann, C. L., Skovgaard, A. M., Olsen, E. M., Larsen, M., . . . Hamann, S. (2017c). Optic Disc Drusen in Children: The Copenhagen Child Cohort 2000 Eye Study. *Journal of Neuro-Ophthalmology, 38*(2), 140-146. doi:10.1097/wno.0000000000000567

Malmqvist, L., Lindberg, A.-S. W., Dahl, V. A., Jørgensen, T. M., & Hamann, S. (2017). Quantitatively Measured Anatomic Location and Volume of Optic Disc Drusen: An Enhanced Depth Imaging Optical Coherence Tomography Study. *Investigative Ophthalmology & Visual Science, 58*(5), 2491. doi:10.1167/iovs.17-21608

Malmqvist, L., Lund-Andersen, H., & Hamann, S. (2017). Long-term evolution of superficial optic disc drusen.(Report). *Acta Ophthalmologica, 95*(4), 352. doi:10.1111/aos.13315

Malmqvist, L., Sibony, P. A., Fraser, C. L., Wegener, M., Heegaard, S., Skougaard, M., . . . Wong, S. H. (2018). Peripapillary Ovoid Hyperreflectivity in Optic Disc Edema and Pseudopapilledema. *Ophthalmology, 125*(10), 1662-1664. doi:10.1016/j.ophtha.2018.04.036

Medical, T. (2016). 3D OCT-1 Maestro. Retrieved from http://www.topconmedical.com/products/3doct1maestro.htm

Merchant, K. Y., Su, D., Park, S. C., Qayum, S., Banik, R., Liebmann, J. M., & Ritch, R. (2013). Enhanced Depth Imaging Optical Coherence Tomography of Optic Nerve Head Drusen. *Ophthalmology, 120*(7), 1409-1414. doi:https://doi.org/10.1016/j.ophtha.2012.12.035

Min Lee, K., Woo, S. J., & Hwang, J.-M. (2013). *Morphologic Characteristics of Optic Nerve Head Drusen on Spectral-Domain Optical Coherence Tomography* (Vol. 155).

Nagata, S. (1997). Apoptosis by Death Factor. *Cell, 88*(3), 355-365. doi:https://doi.org/10.1016/S0092-8674(00)81874-7

Naing, L., Winn, T., & Nordin, R. (2006). Pratical Issues in Calculating the Sample Size for Prevalence Studies. *Archives of Orofacial Sciences, 1*.

Nolan, K. W., Lee, M. S., Jalalizadeh, R. A., Firl, K. C., Van Stavern, G. P., & McClelland, C. M. (2017). Optic Nerve Head Drusen: The Relationship Between Intraocular Pressure and Optic Nerve Structure and Function. *J Neuroophthalmol, 38*(2), 147-150. doi:10.1097/wno.0000000000000587

Partha, C. K., Guoqing, D., Yu, F., Daxi, S., Janardhan, S., Kelly, E. M., . . . John, D. S. (2006). Identification of a mammalian mitochondrial porphyrin transporter. *Nature, 443*(7111), 586. doi:10.1038/nature05125

Pineles, S. L., & Arnold, A. C. (2012). Fluorescein angiographic identification of optic disc drusen with and without optic disc edema. *J Neuroophthalmol, 32*(1), 17-22. doi:10.1097/WNO.0b013e31823010b8

Purvin, V., King, R., Kawasaki, A., & Yee, R. (2004). Anterior ischemic optic neuropathy in eyes with optic disc drusen. *Arch. Ophthalmol., 122*(1), 48-53.

Rebolleda, G., Diez-Alvarez, L., Casado, A., Sánchez-Sánchez, C., de Dompablo, E., González-López, J. J., & Muñoz-Negrete, F. J. (2015). OCT: New perspectives in neuro-ophthalmology. *Saudi Journal of Ophthalmology, 29*(1), 9-25. doi:10.1016/j.sjopt.2014.09.016

Roh, S., Noecker, R. J., Schuman, J. S., Hedges, T. R., Weiter, J. J., & Mattox, C. (1998). Effect of optic nerve head drusen on nerve fiber layer thickness11The authors have no proprietary interest in the development of this or competing instruments. *Ophthalmology, 105*(5), 878-885. doi:https://doi.org/10.1016/S0161-6420(98)95031-X

Sakamoto, A., Hangai, M., & Yoshimura, N. (2008). Spectral-Domain Optical Coherence Tomography with Multiple B-Scan Averaging for Enhanced Imaging of Retinal Diseases. *Ophthalmology, 115*(6), 1071-1078.e1077. doi:10.1016/j.ophtha.2007.09.001

Sato, T., Mrejen, S., & Spaide, R. F. (2013). Multimodal Imaging of Optic Disc Drusen. *American Journal of Ophthalmology, 156*(2), 275-282.e271. doi:10.1016/j.ajo.2013.03.039

Schmitz-Valckenberg, S., Holz, F. G., Bird, A. C., & Spaide, R. F. (2008). Fundus autofluorescence imaging: review and perspectives. *Retina, 28*(3), 385-409. doi:10.1097/IAE.0b013e318164a907

Skaat, S. A., Muylaert, L. S., Mogil, F. R., Furlanetto, M. R., Netto, C. C., Banik, C. R., . . . Park, C. S. (2017). Relationship Between Optic Nerve Head Drusen Volume and Structural and Functional Optic Nerve Damage. *Journal of Glaucoma, 26*(12), 1095-1100. doi:10.1097/IJG.0000000000000783

Skougaard, M., Heegaard, S., Malmqvist, L., & Hamann, S. (2019). Prevalence and histopathological signatures of optic disc drusen based on microscopy of 1713 enucleated eyes. *Acta Ophthalmologica*. doi:10.1111/aos.14180

Slotnick, S., & Sherman, J. (2012). Buried Disc Drusen Have Hypo-Reflective Appearance on SD-OCT. *Optometry and Vision Science, 89*(5), E704-E708. doi:10.1097/OPX.0b013e31824ee8e0

Teixeira, F. J., Marques, R. E., Mano, S. S., Couceiro, R., & Pinto, F. (2019). Optic disc drusen in children: morphologic features using EDI-OCT. *Eye (London, England)*. doi:10.1038/s41433-019-0694-6

TNRPA. (2012). Veileder for bruk av optisk stråling til medisinsk og kosmetisk behandling. In (pp. 9-10): THE NORWEGIAN RADIATION PROTECTION AUTHORITY.

Tsikata, C. E., Vercellin Verticchio, Y.-C. A., Falkenstein, B. I., Poon, C. L., Brauner, C. S., Khoueir, C. Z., . . . Chen, C. T. (2017). Volumetric Measurement of Optic Nerve Head Drusen Using Swept-Source Optical Coherence Tomography. *Journal of Glaucoma, 26*(9), 798-804. doi:10.1097/IJG.0000000000000707

Tso, M. O. M. (1981). Pathology and Pathogenesis of Drusen of the Optic Nervehead. *Ophthalmology, 88*(10), 1066-1080. doi:10.1016/S0161-6420(81)80038-3

Wang, D. D., Leong, J. C. Y., Gale, J., & Wells, A. P. (2018). Multimodal imaging of buried optic nerve head drusen. *Eye, 32*(6), 1145-1146. doi:10.1038/s41433-017-0009-8

Wilkins, J. M., & Pomeranz, H. D. (2004). Visual manifestations of visible and buried optic disc drusen. *J Neuroophthalmol, 24*(2), 125-129.

Yi, A. K., Mujat, T. M., Sun, G. W., Burnes, A. D. D., Latina, H. M., Lin, F. D., . . . Chen, C. T. (2009). Imaging of Optic Nerve Head Drusen: Improvements With Spectral Domain

Optical Coherence Tomography. *Journal of Glaucoma, 18*(5), 373-378.
doi:10.1097/IJG.0b013e31818624a4

You, Q. S., Xu, L., Wang, Y. X., & Jonas, J. B. (2009). Prevalence of optic disc drusen in an adult Chinese population: the Beijing Eye Study. *Acta Ophthalmologica, 87*(2), 227-228.
doi:10.1111/j.1755-3768.2008.01211.x

List of figures and tables

Annexes

Annex 1: Consent form that were given to participants that signed if they approved.

FOREKOMST AV OPTISK DISKDRUSER I EN NORSK OPTOMETRISK PRAKSIS

Dette er et spørsmål til deg om å delta i et forskningsprosjekt for å undersøke forekomst av optisk diskdruser som er en type forandring som skjer i synsnerven hos noen personer. Disse diskdrusene er sjeldne, men kan forekomme på forskjellige nivåer i synsnerven. Ved bruk av et instrument (OCT, optisk koherens tomograf) kan vi oppdage diskdruser som ligger dypere i synsnerven, og ikke kun de overfladiske som en ser ved netthinneundersøkelse (oftalmoskopi eller netthinnefotografering). Diskdruser i synsnerven er ufarlige, men kan føre til at synsfeltet blir noe redusert på grunn av press mot nervefibrene som går gjennom synsnerven. Tilstanden kan forveksles med hevelse i synsnerven som krever umiddelbar behandling. Resultatene av studien forventes å bidra til økt kunnskap om forekomst av diskdruser blant personer som besøker optiker i Norge. Å vite mer om diskdruser kan være en viktig faktor i å utvikle et bedre system for tidlig identifisering, og vil gi informasjon som fører til bedre kliniske prosedyrer og retningslinjer for optikere.

Du er valgt ut til å være med på bakgrunn av at du har kommet til synsundersøkelse og er over 18 år. Studien er en del av et masterprosjekt, og den ansvarlige for studien er førsteamanuensis Tove Lise Morisbakk ved avdeling for optometri, radiografi og lysdesign ved Universitetet i Sørøst-Norge.

6   HVA INNEBÆRER PROSJEKTET?

Du vil gjennomgå en standard synsundersøkelse som er etter retningslinjene til Norges Optikerforbund. Dette innebærer blant annet: innledende samtale og spørsmål, måling av synsevne, vurdering av samsyn, utmåling av eventuelle synsfeil på avstand og nær, samt mikroskopiundersøkelse av fremre og bakre del av øynene. Det vil i tillegg bli målt øyetrykk samt tatt foto av netthinnen. Undersøkelsen som er spesifikk for denne studien består av en måling med et instrument (optisk koherens tomografi) som foretar en skanning av synsnerven. Tidsforbruket vil for denne målingen være ca. 5-10 minutter i tillegg til den ordinære synsundersøkelsen. Dersom pupillene dine er små, må vi dryppe øynene dine med pupilleutvidende dråper.

I prosjektet vil vi innhente og registrere opplysninger om deg. Personalia samt resultater fra den ordinære synsundersøkelsen og alle bilder som blir tatt, vil bli lagret i klinikkens eget journalsystem med gjeldene lovverk for lagring av pasientopplysninger og taushetsplikt. Opplysninger relatert til studien vil bli avidentifisert og lagret eksternt. De opplysninger som registreres om deg i studien er kjønn, alder, brillestyrke, eventuelle sykdommer, øyehelse og medikamentbruk, samt resultater fra netthinneundersøkelsen. Disse avidentifiserte opplysningene vil bli lagret i 5 år etter prosjektet er avsluttet.

7 MULIGE FORDELER OG ULEMPER

Som deltaker i prosjektet får du en grundig undersøkelse av netthinnen og synsnerven din. Synsnerven er meget viktig for synet ditt, og vi kan med denne undersøkelsen oppdage eventuelle uregelmessigheter. Dersom det oppdages noen unormale funn vil vi følge opp dette og sørge for at du får informasjon og eventuell henvisning til øyelege. Undersøkelsen medfører ingen ubehag, men noe ekstra tidsbruk påberegnes. For enkelte deltakere vil det være nødvendig å bruke øyedråper (Tropikamid 0,5% minims) for å utvide pupillene. Dette kan av noen oppleves litt ubehagelig da dråpene kan svi noe, samt at man blir mer lysømfintlig i etterkant. Effekten av øyendråpene vil avta gradvis og opphører helt etter noen timer.

8 FRIVILLIG DELTAKELSE OG MULIGHET FOR Å TREKKE SITT SAMTYKKE

Det er frivillig å delta i prosjektet. Dersom du ønsker å delta, undertegner du samtykkeerklæringen på siste side. Du kan når som helst og uten å oppgi noen grunn trekke ditt samtykke. Dette vil ikke få konsekvenser for din videre behandling hos Krogh Optikk. Du har full innsynsrett i de opplysninger som er registrert om deg. Du har også rett til å få innsamlede helse- og personopplysninger slettet eller utlevert. Unntaket for dette vil være dersom de innsamlede opplysningene allerede inngår i publiserte vitenskapelige arbeider, eller dersom datamaterialet allerede er anonymisert. (Helsedepartementets rundskriv 1/10-2003)

Dersom du senere ønsker å trekke deg eller har spørsmål til prosjektet, kan du kontakte **Marte Roti, tlf. 22 95 79 70, Kirkeveien 64, 0364 OSLO**, eller e-post: marteroti@hotmail.com.

9 HVA SKJER MED INFORMASJONEN OM DEG?

Informasjonen som registreres om deg skal kun brukes slik som beskrevet i hensikten med studien. Du har rett til innsyn i hvilke opplysninger som er registrert om deg og rett til å få korrigert eventuelle feil i de opplysningene som er registrert.

Alle opplysningene vil bli behandlet uten navn og fødselsnummer eller andre direkte gjenkjennende opplysninger. En koblingskode vil knytte deg til dine opplysninger gjennom en navneliste. Navnelisten og kodene vil bli oppbevart adskilt.

Prosjektleder har ansvar for den daglige driften av forskningsprosjektet og at opplysninger om deg blir behandlet på en sikker måte. Informasjon om deg vil bli avidentifisert eller slettet senest fem år etter prosjektslutt.

10 GODKJENNING

Prosjektet er godkjent av Regional komite for medisinsk og helsefaglig forskningsetikk, 2018/1656.

Etter ny personopplysningslov har behandlingsansvarlig, Universitetet i Sørøst-Norge, og prosjektleder Marte Roti, et selvstendig ansvar for å sikre at behandlingen av dine opplysninger har et lovlig grunnlag. Dette prosjektet har rettslig grunnlag i EUs personvernforordning artikkel 6a og artikkel 9 nr. 2 og ditt samtykke.

Du har rett til å klage på behandlingen av dine opplysninger til Datatilsynet.

11 KONTAKTOPPLYSNINGER

Dersom du har spørsmål til prosjektet kan du ta kontakt med **Marte Roti, tlf. 22 95 79 70, Kirkeveien 64, 0364 OSLO**, eller e-post: marteroti@hotmail.com.

Personvernombud ved institusjonen er Paal Are Solberg (Paal.A.solberg@usn.no).

12 SAMTYKKE TIL DELTAKELSE I PROSJEKTET

13 JEG ER VILLIG TIL Å DELTA I PROSJEKTET

---   ---
Sted og dato   Deltakers signatur

                                                                   Deltakers navn med trykte bokstaver

Jeg bekrefter å ha gitt informasjon om prosjektet.

---   ---
Sted og dato   Signatur